iScience

CellPress
OPEN ACCESS

Article

Development of novel cytoprotective small compounds inhibiting mitochondria-dependent cell death

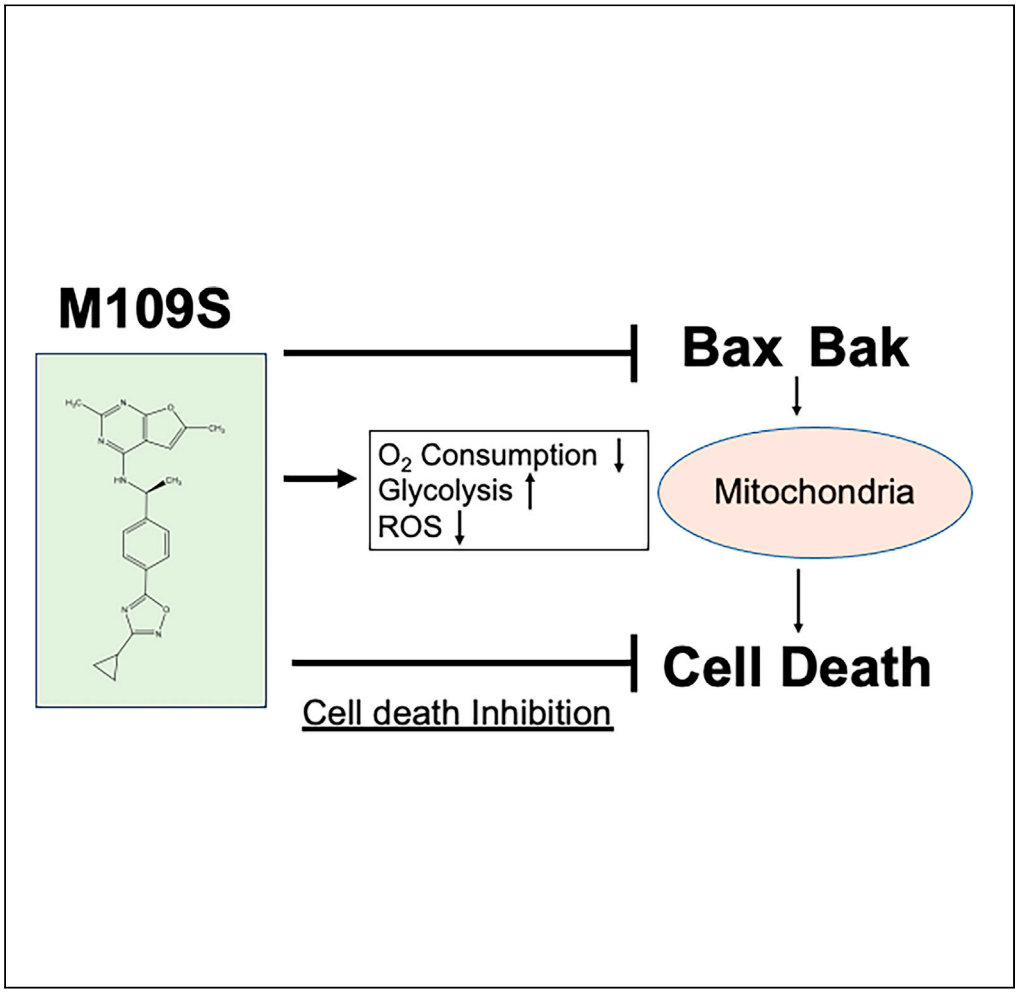

Mieko Matsuyama, Joseph T. Ortega, Yuri Fedorov, ..., Beata Jastrzebska, William Greenlee, Shigemi Matsuyama

shigemi.matsuyama@case.edu

Highlights

M109S inhibits Bax-/Bak-dependent cell death (except certain types of cancer cells)

Orally administered M109S protected the mouse retina from bright-light-induced cell death

M109S binds Bax and inhibits the translocation of Bax from the cytosol to mitochondria

M109S decreases cellular oxygen usage and ROS levels, whereas it increases glycolysis

Matsuyama et al., iScience *26*, 107916
October 20, 2023
https://doi.org/10.1016/j.isci.2023.107916

iScience

CellPress
OPEN ACCESS

Article

Development of novel cytoprotective small compounds inhibiting mitochondria-dependent cell death

Mieko Matsuyama,[1] Joseph T. Ortega,[2] Yuri Fedorov,[3] Jonah Scott-McKean,[1,4] Jeannie Muller-Greven,[5] Matthias Buck,[5] Drew Adams,[3] Beata Jastrzebska,[2] William Greenlee,[6] and Shigemi Matsuyama[1,2,7,8,9,10,*]

SUMMARY

We identified cytoprotective small molecules (CSMs) by a cell-based high-throughput screening of Bax inhibitors. Through a medicinal chemistry program, M109S was developed, which is orally bioactive and penetrates the blood-brain/retina barriers. M109S protected retinal cells in ocular disease mouse models. M109S directly interacted with Bax and inhibited the conformational change and mitochondrial translocation of Bax. M109S inhibited ABT-737-induced apoptosis both in Bax-only and Bak-only mouse embryonic fibroblasts. M109S also inhibited apoptosis induced by staurosporine, etoposide, and obatoclax. M109S decreased maximal mitochondrial oxygen consumption rate and reactive oxygen species production, whereas it increased glycolysis. These effects on cellular metabolism may contribute to the cytoprotective activity of M109S. M109S is a novel small molecule protecting cells from mitochondria-dependent apoptosis both *in vitro* and *in vivo*. M109S has the potential to become a research tool for studying cell death mechanisms and to develop therapeutics targeting mitochondria-dependent cell death pathway.

INTRODUCTION

The Bcl-2 family of proteins is a group of evolutionarily conserved proteins regulating mitochondria-dependent apoptosis (reviewed in[1]). The abnormal balance of these proteins induces apoptosis resistance of cancer cells and unwanted apoptosis of essential cells in the damaged tissues.[1] Bax and Bak are the pro-apoptotic members of the Bcl-2 family of proteins playing a central role in the mitochondria-dependent programmed cell death.[2] Because Bax/Bak double-deficient cells are resistant to the stresses activating the mitochondria-dependent apoptosis pathway,[2] Bax and Bak are ideal pharmacological targets to control the life and death of the cells. The pharmacological activators and inhibitors of Bax and Bak are expected to be effective in eliminating cancer cells and rescuing essential cells from unwanted death, respectively.[3–7]

Previously, small compounds activating Bax-/Bak-dependent apoptosis pathway have been developed, and some of these small compounds are used clinically as effective therapeutics eliminating cancer cells, for example, venetoclax.[8,9] However, clinically effective small compounds rescuing damaged cells from Bax-/Bak-induced cell death have not yet been developed. Previous studies have reported the development of Bax-inhibiting compounds (pro-drugs) by identifying small molecules inhibiting the pore forming activity of Bax in synthetic liposome, for example, Bax channel blocker (Compound 1),[10] iMac2,[10,11] and MSN-125.[12] Bax channel blocker (Compound 1)[10] was also reported to have an activity to inhibit the conformational change of Bax, and it is also called Bax activation inhibitor-1 (BAI-1).[13] These inhibitors showed cell death inhibiting activities in cell culture, but its activity in animal disease models has not been well studied. Recently, eltrombopag, an FDA-approved drug for thrombocytopenia, was found to possess direct Bax-binding and -inhibiting activity.[14] For example, eltrombopag inhibited ABT-263-induced cell death in cultured NIH3T3 mouse fibroblasts (EC_{50} = 525 nM).[14] These previous studies developing Bax inhibitors were conducted by using an artificially reconstituted *in vitro* assay system. The compounds identified by *in vitro* assay system will have the expected biochemical activity; however, there is no guarantee that they will have the expected efficacy in living cells without unexpected toxic effects.

[1]Department of Ophthalmology and Visual Science, School of Medicine, Case Western Reserve University, Cleveland, OH 44106, USA
[2]Department of Pharmacology and Cleveland Center for Membrane and Structural Biology, School of Medicine, Case Western Reserve University, Cleveland, OH 44106, USA
[3]Department of Genetics and Genome Science, School of Medicine, Case Western Reserve University, Cleveland, OH 44106, USA
[4]Department of Macromolecular Science and Engineering, School of Engineering, Case Western Reserve University, Cleveland, OH 44106, USA
[5]Department of Physiology and Biophysics, School of Medicine, Case Western Reserve University, Cleveland, OH 44106, USA
[6]Harrington Discovery Institute, Cleveland, OH 44106, USA
[7]Department of Pathology, School of Medicine, Case Western Reserve University, Cleveland, OH 44106, USA
[8]Division of Hematology and Oncology, Department of Medicine, School of Medicine, Case Western Reserve University, Cleveland, OH 44106, USA
[9]Case Comprehensive Cancer Center, Cleveland, OH 44106, USA
[10]Lead contact
*Correspondence: shigemi.matsuyama@case.edu
https://doi.org/10.1016/j.isci.2023.107916

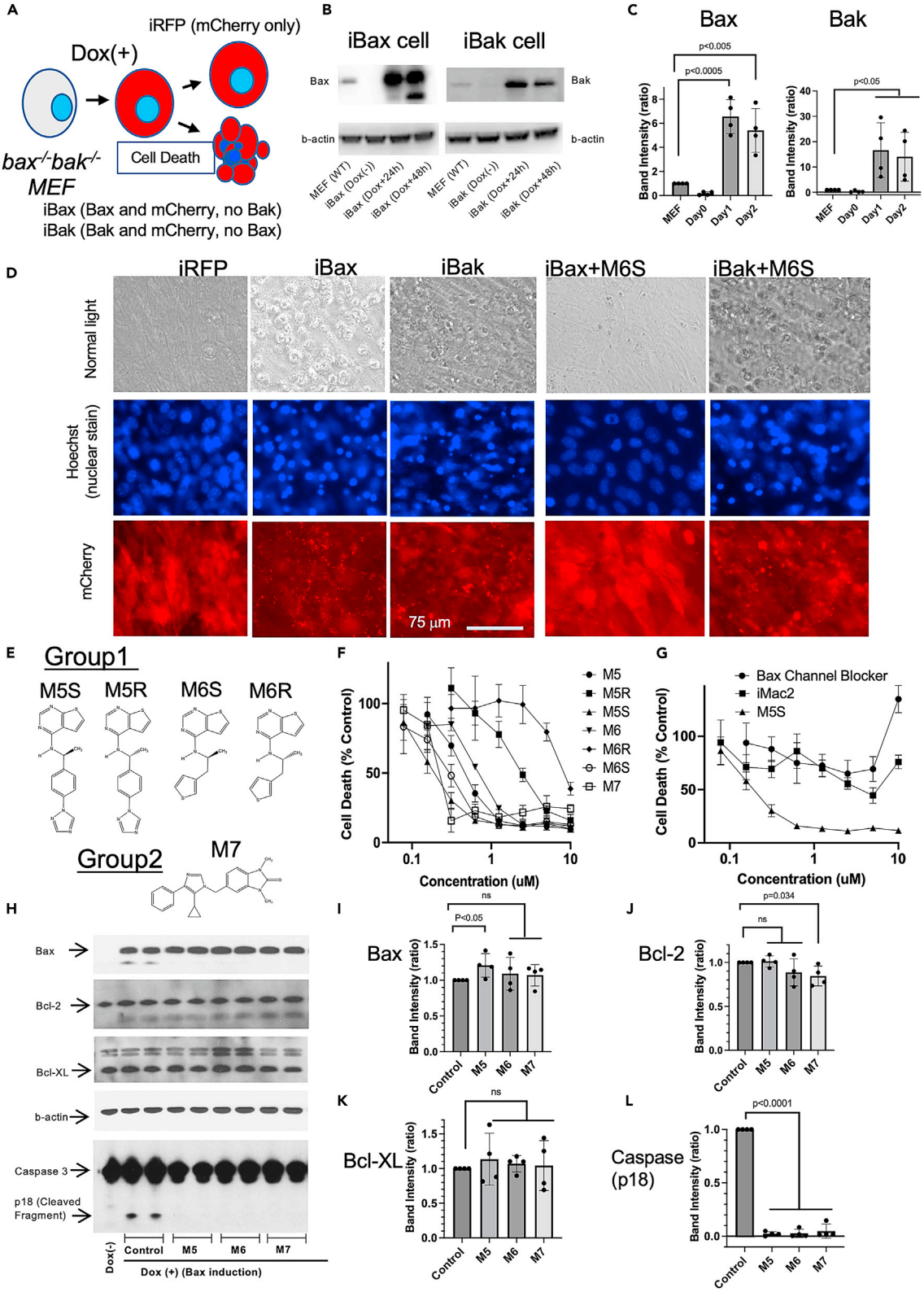
A
iRFP (mCherry only)
Dox(+)
bax-/-bak-/- MEF
Cell Death
iBax (Bax and mCherry, no Bak)
iBak (Bak and mCherry, no Bax)
B
iBax cell
iBak cell
Bax
Bak
b-actin
MEF (WT)
iBax (Dox(-))
iBax (Dox+24h)
iBax (Dox+48h)
iBak (Dox(-))
iBak (Dox+24h)
iBak (Dox+48h)
C
Bax
Bak
p<0.005
p<0.0005
p<0.05
Band Intensity (ratio)
MEF
Day0
Day1
Day2
D
iRFP
iBax
iBak
iBax+M6S
iBak+M6S
Normal light
Hoechst (nuclear stain)
mCherry
75 μm
E
Group1
M5S
M5R
M6S
M6R
Group2
M7
F
Cell Death (% Control)
Concentration (uM)
M5
M5R
M5S
M6
M6R
M6S
M7
G
Bax Channel Blocker
iMac2
M5S
H
Bax
Bcl-2
Bcl-XL
b-actin
Caspase 3
p18 (Cleaved Fragment)
Dox(-)
Control
M5
M6
M7
Dox (+) (Bax induction)
I
Bax
ns
P<0.05
J
Bcl-2
p=0.034
K
Bcl-XL
L
Caspase (p18)
p<0.0001

Figure 1. Development of Bax- or Bak-inducible system in *bax*$^{-/-}$*bak*$^{-/-}$ MEFs and the screening of small compounds rescuing cells from Bax or Bak

(A) Doxycycline (Dox)-induced expression of Bax and Bak in MEFs. Dox-inducible Bax or Bak (no-tag) gene was introduced in *bax*$^{-/-}$*bak*$^{-/-}$ MEFs by lentivirus vectors. These cells were named iBax or iBak cells, respectively. The cells expressing only mCherry were named iRFP cells.

(B and C) Western blot analysis of the expression levels of Bax or Bak in wild-type (*Wt*) MEFs, iBax, and iBak cells are shown (B). The results of densitometric analyses are shown in C. The expression levels of Bax and Bak in *Wt* MEFs were designated as 1 (actin levels were used as loading control). The result of the t test statistical analysis is shown. Statistically significant difference ($p < 0.05$) is indicated in the figure. Data are presented as mean ± SD.

(D) Cell images of iRFP, iBax, and iBak. The Dox-inducible mCherry (red fluorescent protein) gene was introduced in *bax*$^{-/-}$*bak*$^{-/-}$ to monitor Dox-inducible gene expression. Pictures were taken 48 h after Dox addition (100 ng/mL) to the medium. Images show cells under normal light, stained with Hoechst dye (nuclear staining), and expressing mCherry. Cell death (nuclear condensation and fragmentation), as well as apoptotic bodies (mCherry images), can be observed in these images. M6S is one of the hit compounds suppressing Bax-induced cell death. M6S (1 μM) rescued iBax cells, but not iBak cells.

(E) Chemical structures of hit compounds are shown.

(F) The dose-dependent inhibition of Bax-induced apoptosis in iBax cells by M5, M6, and M7 that were the best three representative hit compounds. The % of apoptosis was measured by the detection of apoptotic nuclei by Hoechst dye nuclear staining. The enantiomer S form of M5 and M6 (M5S and M6S) showed significantly stronger activities than the enantiomer R form (M5R and M6R). The original compounds in the library (M5 and M6) were a mixture of S and R forms with unknown ratio. Data are presented as mean ± SD.

(G) The dose-dependent effects of M5S, iMac2, and Bax channel blocker suppressing cell death in iBax system is shown. M5S showed significantly stronger activity than iMac2 and Bax channel blocker inhibiting cell death in iBax cells. Data are presented as mean ± SD.

(H–L) Western blot analysis of Bcl-2 family proteins and Caspase-3 in iBax cells treated with M5, M6, and M7. iBax cells were incubated for 48 h with or without Dox (100 ng/mL) in the presence or absence of M5, M6, or M7. M5 and M6 are the original hit compounds that are a mixture of R and S forms. The results of the densitometric analysis are shown on the right as graphs. The expression level of each protein in the control group is designated as 1 (actin levels were used as loading control). All the compounds suppressed Caspase-3 cleavage without major changes in the expression levels of Bax, Bcl-2, and Bcl-XL. The result of the t test statistical analysis is shown in each graph. "ns": no statistically significant difference was detected ($p > 0.05$). Data are presented as mean ± SD.

In this study, we utilized the cell-based functional screening system to develop novel cytoprotective small molecules (CSMs) that rescue cells from Bax-induced apoptosis. The chemical structures of CSMs, described here, are distinct from previously reported Bax inhibitors identified through the reconstituted *in vitro* system. Through medicinal chemistry efforts, we succeeded in developing M109S, which has favorable pharmacokinetics in rodents. In this article, we report the chemical structures of CSMs and their activities protecting cells at the levels of cell culture and mouse retinal disease models.

RESULTS

Development of cell-based Bax/Bak inhibitor screening system

We generated cell lines that undergo apoptosis by the expression of Bax or Bak in *bax*$^{-/-}$*bak*$^{-/-}$ mouse embryonic fibroblasts (MEFs). In these cells, the Tet-ON promoter[15] is used for the induction of mCherry (red fluorescent protein), Bax, and Bak (Bax and Bak are expressed without mCherry-tag). Therefore, expression levels of Bax and Bak can be indirectly monitored by mCherry's red fluorescence intensity. These cells were named iRFP (mCherry-inducible cells), iBax (Bax-inducible cells), or iBak (Bak-inducible cells) (Figures 1A–1C).

Doxycycline (Dox), a tetracycline analog, was used to activate the Tet-ON system, and the expression of Bax and Bak was confirmed by Western blot (Figures 1B and 1C). Forty-eight hours after the induction, many apoptotic cells can be observed by microscopic analysis (Figure 1D). To detect apoptotic nuclei, cells were stained with Hoechst dye (Figure 1D). These iBax cells were used to identify the candidates of CSMs. A 50,000 small compound library was used to identify hit compounds by using a cell image analysis system (Operetta system, PerkinElmer). The hits were selected by the following two criteria: (1) decreasing the percentage of dead cells detected (nuclear fragmentation and condensation) and (2) maintaining mCherry expression (fluorescence intensity) above 80% of the control so that compounds inhibiting the Tet-ON system could be excluded. We then selected the top 50 compounds that satisfied these criteria. Based on similarities in the chemical structure, the compounds were divided into 2 groups. The best three small molecules rescuing iBax cells were M5, M6, and M7 (Figure 1E). M5 and M6 (that have two enantiomers R and S) were assigned to Group 1 and M7 to Group 2. Figure 1D shows an example of M6S protecting iBax cells from Bax-induced apoptosis while maintaining mCherry expression. These Bax-inhibiting hits were then tested in iBak cells. However, none of these compounds were able to inhibit cell death induced by the overexpression of Bak in iBak cells (Figure 1D, example images of iBax and iBak cells incubated with M6S 1 μM are shown). These results suggest that CSMs can rescue cells from the apoptotic processes induced by the overexpression of Bax but not Bak. The dose-response effects of M5, M5R, M5S, M6, M6R, M6S, and M7 inhibiting Bax-induced apoptosis in iBax cells are shown in Figure 1F. The S-enantiomer showed a significantly higher cell-death-inhibiting activity than the R-form in both M5 and M6. Therefore, we focused on the S-enantiomer to perform Hit-to-Lead optimization in Group 1. To be noted, the cell death inhibition activity of M5S is significantly higher than the activities of Bax channel blocker[10] and iMac2[10,11](Figure 1G). Western blot analyses showed that these compounds did not decrease Bax expression (Figures 1H and 1I) but rather suppressed Caspase-3 activation (cleavage) (Figures 1H and 1L). The expression levels of endogenous Bax inhibitors such as Bcl-2 and Bcl-XL did not show major changes (Figures 1J and 1K).

Hit-to-lead optimization

A medicinal chemistry program was carried out to expand the two-lead series and optimize iBax cell potency and Bax binding. A total of 200 inhibitors were designed and synthesized.[16] Among them, M41S (Series 1) and M11 (Series 2) were the best apoptosis inhibitors in iBax cells

(Figures 2A–2C). The EC_{50} of M41S and M11 for the inhibition of caspase activation in iBax cells were 3.8 nM (Figure 2D) and 145 nM (Figure 2C), respectively. In comparison with the original hit compounds of M5 (S (EC_{50} = 124 nM) and R (EC_{50} = 1,450 nM)) and M7 (EC_{50} = 553 nM), apoptosis-inhibiting activities of M41S and M11 were significantly improved (Figures 2B–2D). Further optimization of the lead compound M41S (Series 1) led to the identification of M109S, an advanced lead compound, protecting iBax cells with the EC_{50} of 23.4 nM (Figures 2A and 2D). M109S exhibits drug-like profiles: molecular weight is 375 g/mol, cLogP = 4.0, kinetic solubility is 0.05 μM in pH 7.4 (clear suspension/solution can be prepared in 15% beta-cyclodextrin solution at 2 mg/mL [5.33 mM]), Caco-2 cell permeability is 11.7 × 10^{-6} cm/s and the efflux ratio is 1.3, microsomal stability (half-life [t ½]) is 46 min (human) or 11 min (mouse), and plasma protein binding is 99.97% (human) or 99.71 (mouse). The detail synthesis protocols and pathways for M109S has been published.[16] As shown in Figure 2D, the apoptosis inhibition activity of M41S and M109S in iBax cells is significantly higher than the activity of eltrombopag, a thrombopoietin receptor analog, which is recently reported to have Bax inhibitor activity.[14] We also tried optimization of the lead compound M11 (Series 2); however, we were not able to obtain an advanced lead compound passing the drug profiling tests suitable for human and animal use within the three-year project period.

M109 is an orally bioactive cell death inhibitor penetrating blood-brain/retina-barrier

The pharmacokinetic (PK) analysis of M109S was performed in both mice and rats by oral gavage (PO) and either by intraperitoneal (IP) or by intravenous (IV) injection (Figures 2E–2G). In mice, M109S reached 1.0 μg/mL (2.6 μM) plasma concentration within 30 min from administration, and it remained at 596 ± 134 ng/mL (1.6 ± 0.36 μM) 24 h after the oral gavage administration (Figure 2E). Similar results were obtained in rats (Figure 2F). At 24 h after the oral gavage administration, the level of M109S in the plasma was 565.3 ± 188.3 nM in rats. Moreover, M109S crossed the blood-brain and blood-retina barriers. The level of M109S in the rat retina and brain reached 171.0 ± 52.0 nM and 222.7 ± 74.7 nM, respectively, 24 h after its oral administration (Figures 2F and 2G). Notably, these concentrations are higher than the EC_{50} concentration (23.4 nM) of M109S protecting iBax cells (Figure 2D). The half-life ($t_{1/2}$) of M109S (10 mg/kg body weight [b.w.] oral administration) in the blood was longer than 12 h (in mice) or 9.7 h (in rats) (Figures 2E and 2F).

M109S protected the retina from the bright-light-induced photoreceptor death

Previous studies showed that Bax-mediated apoptosis plays an essential role in bright-light-induced retinal degeneration in *Abca4*$^{-/-}$*Rdh8*$^{-/-}$ mice.[17] *Abca4*$^{-/-}$*Rdh8*$^{-/-}$ mouse is a mouse model of human Stargardt disease, a juvenile age-related macular degeneration (AMD) that is susceptible to acute light insult and the retinal degeneration.[17–19] The retinal photoreceptor cells degenerate within 7 days in these mice after illumination with bright light due to apoptosis. An oral administration of these mice with a total of four doses of M109S at 10 mg/kg within a scheme of two doses before light exposure (24 h and 1h), followed by two doses after light exposure (24 h and 48 h), produced protection of photoreceptor cells from death (Figures 3A–3H). The apoptotic processes occurring in the photoreceptor cells upon bright light injury trigger the activation of an immune response, which correlates with an increased number of autofluorescence (AF) spots in the retina. The AF spots that can be detected with Scanning Laser Ophthalmoscopy (SLO) imaging represent the activated resident microglia and peripheral immune cells that migrate to the retina to clear dying photoreceptors. The increased number of AF spots was detected only in the vehicle-treated mice. However, in mice treated with M109S at 10 mg/kg, the number of AF spots was similar to that detected in the dark-adapted mice (Figures 3A, 3B, and S1). The loss of photoreceptors in the vehicle-treated mice was evidenced by thinning of the outer nuclear cell layer (ONL) detected by the optical coherence tomography (OCT), whereas the ONL in mice treated with M109S at 10 mg/kg closely reassembled the ONL in unexposed mice (Figures 3C and 3D). Although lower doses were less effective (Figures 3D and S2). The thickness of the ONL was confirmed by histological examination of the H&E-stained retinal sections (Figures 3E and 3G). The outer segments of the rod photoreceptors and cone photoreceptor cells were stained with the anti-rhodopsin antibody and peanut agglutinin (PNA), respectively. The treatment with M109S preserved the structure of the retina by preventing the degeneration of both rod (anti-rhodopsin-stained cells) and cone photoreceptors (PNA-stained cells) triggered by the exposure to bright light. Although only the residual staining of rhodopsin and cone opsin was found in the vehicle-treated mice, the expression of these receptors detected in the M109S-treated mice was comparable with that found in mice unexposed to light (Figure 3F). The protection of the photoreceptor cells was confirmed in non-pigmented *Wt* Balb/cJ mice sensitive to light-induced retinal degeneration (Figures 3H and S3). Although exposure to bright light triggered deterioration of photoreceptor cells in the vehicle-treated mice, oral administration of M109S 24 h and 1 h prior to illumination followed by additional treatment 24 h and 48 h after light exposure protected these mouse retinas. Altogether, these results indicate that M109S protects retinal cells from bright-light-induced death and thus prevents retina degeneration triggered by illumination.

Evaluation of cell death inhibition activities of M109S in cultured cells

Next, we evaluated the effectiveness of M109S inhibiting pharmacologically induced cell death in various cell types. ABT-737 is known to activate Bax-/Bak-dependent apoptosis pathway.[20,21] The effects of M109S against ABT-737-induced apoptosis were examined in MEF cells of wild type (*Wt*) (Figure 4A), *bax*$^{+/+}$*bak*$^{-/-}$ (Bax only) (Figure 4B), and *bax*$^{-/-}$*bak*$^{+/+}$ (Bak only) (Figure 4C). M109S showed a dose-dependent suppression of caspase activation in all three types of MEFs, suggesting that M109S can inhibit apoptosis induced by Bax as well as Bak, which are expressed at endogenous levels. Staurosporine (STS), a pan-kinase inhibitor, is often used as a cytotoxic chemical activating Bax-/Bak-dependent mitochondria-induced apoptosis.[2] M109S inhibited apoptosis induced by STS in MEFs (Figure 4D). Etoposide, a topoisomerase inhibitor, is known to activate DNA-damage-induced cell death involving Bax-/Bak-mediated apoptosis.[22,23] M109S also significantly suppressed apoptosis induced by etoposide in Neruo2a cells (Figure 4E). However, in HeLa cells, M109S showed only slight inhibition (most

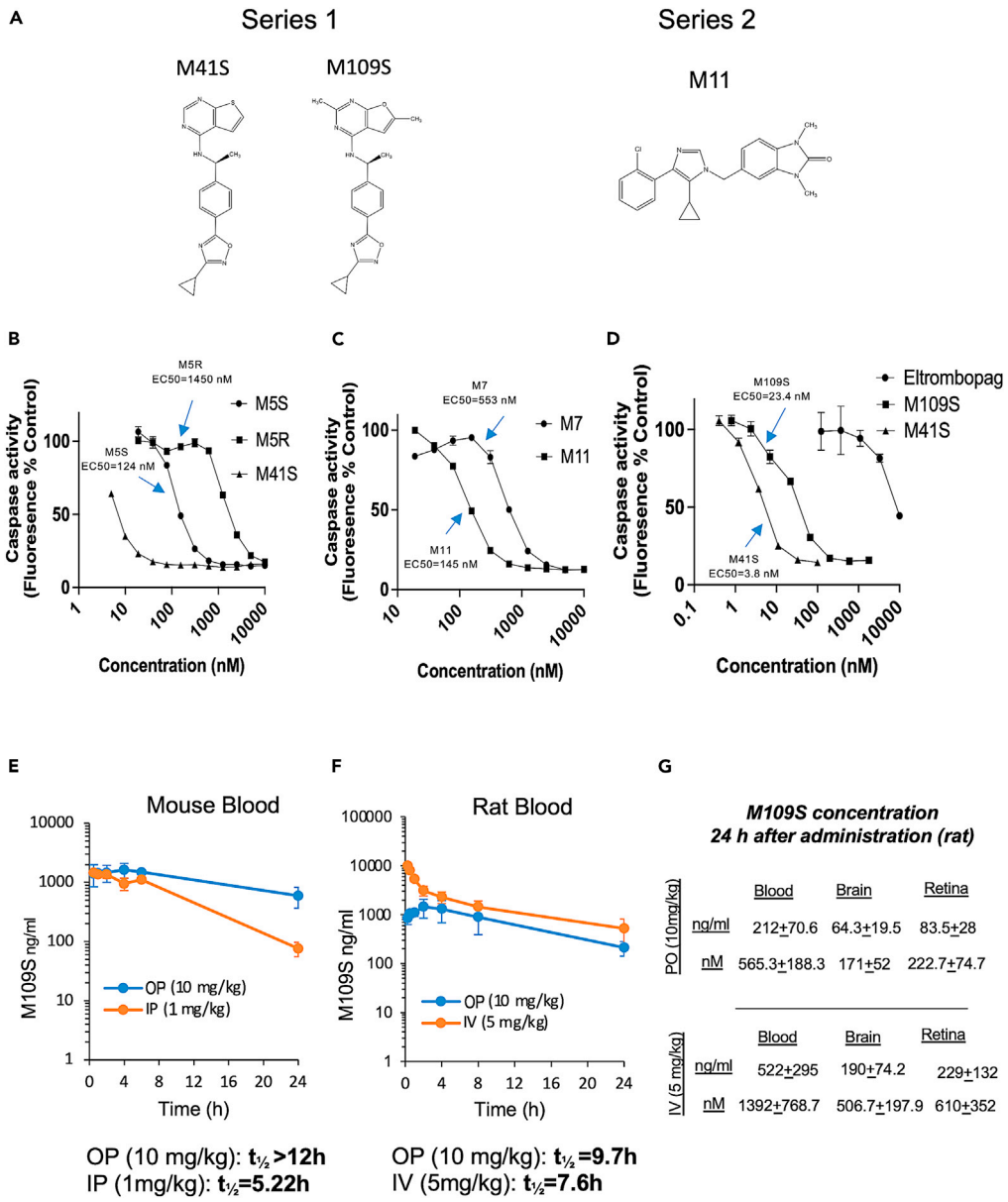

Figure 2. Hit-to-lead optimization of the cytoprotective small molecules (CSMs)

(A) Chemical structures of newly designed and synthesized lead compounds in this study. The most effective cell death inhibitor in cell culture, M41S, was developed based on the common chemical structure of M5S and M6S (Series 1). The orally bioactive CSM, M109S, was developed from M41S. M11 was the most effective cell death inhibitor among the inhibitors designed from M7 (Series 2).

(B–D) Caspase activity of iBax cells treated with CSMs. Bax-mediated apoptosis was induced by Dox addition to the culture medium in iBax cells in the presence of various concentrations of CSMs as indicated in the graphs. The improvement of apoptosis inhibition through Hit-to-lead optimization is shown in (B) (M41S vs. M5S and M5R) and (C) (M11 vs. M7). (D) shows the comparison of M41S (the best cell death inhibitor in cell culture), M109S (orally bioavailable CSM designed from M41S), and eltrombopag (previously reported Bax inhibitor). Data are presented as mean ± SD.

(E–G) Pharmacokinetic analysis of M109S in rodents. M109S was administered to mice and rats by intraperitoneal injection (IP, 1 mg/kg), intravenous injection (IV, 5 mg/kg), or oral gavage (OP, 10 mg/kg). The concentration of M109S was measured by mass spectrometry analysis. G: M109S concentrations in the blood, brain, and retina 24 h after the administration (oral gavage [PO] or intravenous injection [IV]) in rats. Data are presented as mean ± SD.

of the effects were not statistically significant) of etoposide-induced apoptosis (Figures 4F and S4), indicating that M109S inhibits etoposide-induced apoptosis in a cell-type-dependent manner. Obatoclax is known to induce both Bax-/Bak-dependent and independent apoptosis in certain types of cancer cells.[21] M109S inhibited obatoclax-induced apoptosis in ARPE19 cells (human retinal pigment epithelial cell line). M109S suppressed caspase-3 activation without a significant impact on Bax levels of obatoclax-treated ARPE19 cells (Figures 4G–4I).

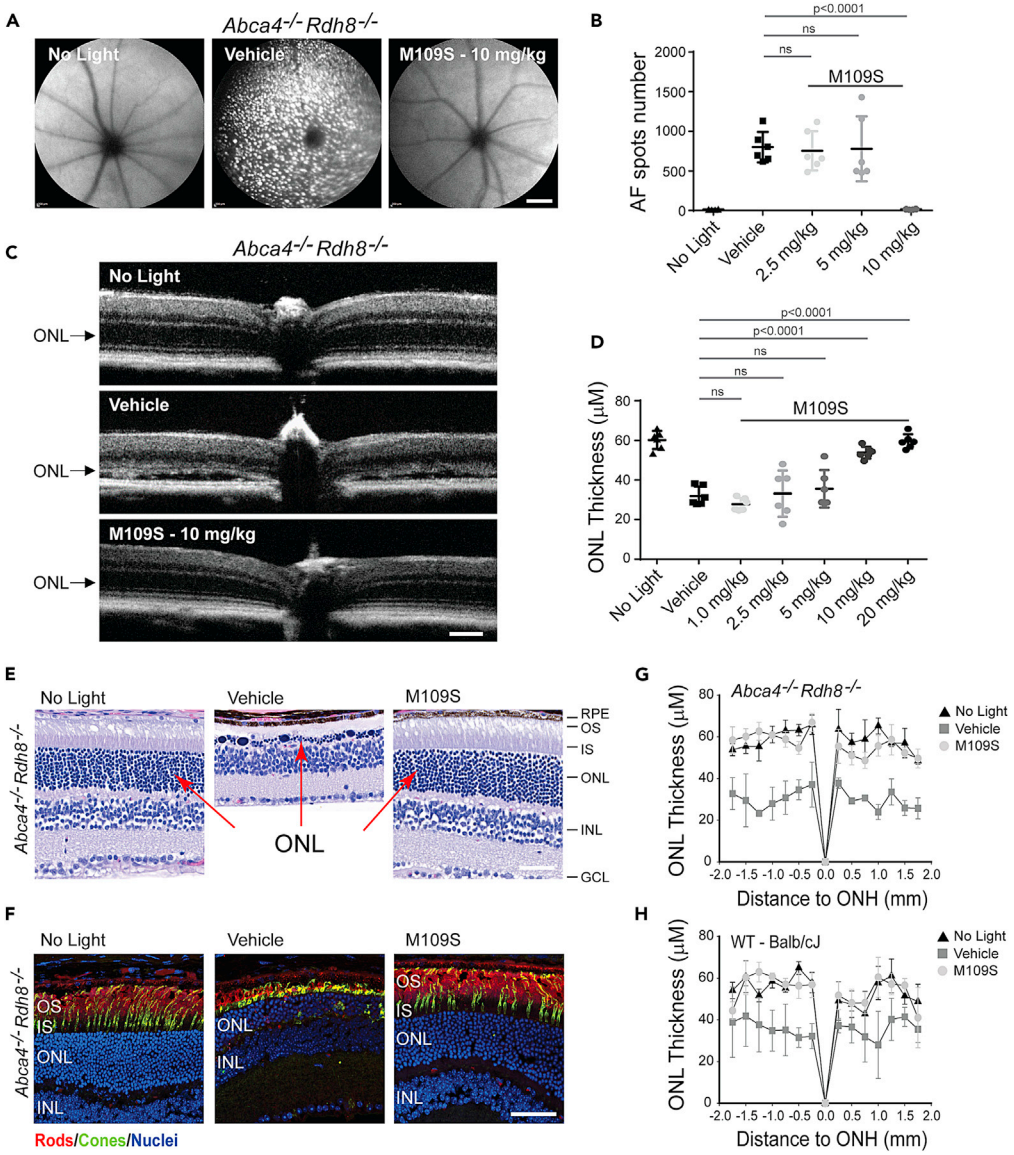

Figure 3. M109S protects the retina from bright-light-induced injury in *Abca4*$^{-/-}$*Rdh8*$^{-/-}$ mice and Balb/cJ mice

(A and B) (A) The *in vivo* whole fundus imaging from *Abca4*$^{-/-}$*Rdh8*$^{-/-}$ mice taken with scanning laser ophthalmoscopy (SLO) one week after exposure to bright light. Autofluorescence spots (AF) representing macrophages and microglial cells activated by light injury to clear dying photoreceptors were detected in only vehicle-treated mice but not in M109S-treated mice (10 mg/kg). Scale bar, 1 mm. (B) Quantification of the AF. M109s at 10 mg/kg showed statistically significant protection against light-induced photoreceptor cell death. Statistical analysis was performed with the one-way ANOVA and post hoc Turkey tests (n = 6 for each group). The values of $p < 0.05$ were considered statistically significant. No statistically significant changes were labeled as "ns".

(C and D) (C) The spectral domain optical coherence tomography (SD-OCT) images of the retina from *Abca4*$^{-/-}$*Rdh8*$^{-/-}$ mice taken one week after illumination. Scale bar, 100 μm. (D) The measurement and statistical analysis of the ONL thickness in SD-OCT images. The exposure to bright light induced the degeneration of photoreceptors, which caused the shortening of the outer nuclear layer (ONL) in retinas in vehicle-treated control mice but not in the M109S-treated group. M109S showed a dose-dependent effect protecting the photoreceptor cells from light-induced death. Statistical analysis was performed with the one-way ANOVA and post hoc Turkey tests (n = 6 for each group). The values of $p < 0.05$ were considered statistically significant. No statistically significant changes were labeled as "ns".

(E) The hematoxylin and eosin (H&E) staining of the retina sections of *Abca4*$^{-/-}$*Rdh8*$^{-/-}$ mice. M109S treatment mitigated degenerative processes in the retina. The thickness of the ONL in mice treated with M109S at 10 mg/kg closely resembled the thickness of the retina in dark-adapted mice. Scale bar, 50 μm. RPE, retinal pigment epithelium; OS, outer segment; IS, inner segment; ONL, outer nuclear layer; INL, inner nuclear layer; GCL, ganglion cell layer.

(F) Histochemical analysis of the retina of *Abca4*$^{-/-}$*Rdh8*$^{-/-}$ mice. The cryosections were stained with an anti-rhodopsin antibody recognizing the C-terminus (1D4 antibody) to detect rod photoreceptors (red) and with peanut agglutinin to detect cone photoreceptors (green). Nuclei were stained with DAPI (blue). M109S treatment prevented the degeneration of both rod and cone photoreceptors. Scale bar, 50 μm.

Figure 3. *Continued*

(G and H) The measurement and statistical analysis of the thickness of the ONL in the H&E-stained sections of the retina of *Abca4*$^{-/-}$*Rdh8*$^{-/-}$ mice (G) and Balb/cJ mice (H). The treatment with M109S (10 mg/kg) prevented the thickening of the ONL caused by the bright light injury in both mouse strains. Data are presented as mean ± SD.

M109S suppressed the conformation change (N-terminal exposure) and the mitochondrial translocation of Bax

The exposure of the N-terminus of Bax occurs as the early step of Bax-induced apoptosis.[24,25] The levels of this conformational change can be examined by immunoprecipitation of Bax by antibodies recognizing the N-terminus of Bax.[24] As shown in Figures 5A and 5B, CSMs (M41S, M11, and M109S) suppressed the conformational change of Bax. Bax is known to translocate from the cytosol to the mitochondria after the conformational change, which could be detected as higher density puncta in control iBax cells labeled with anti-Bax antibody (Figures 5C and 5D).[25] CSMs (M41S, M11, and M109S) suppressed mitochondrial translocation of Bax in iBax cells (Figures 5C and 5D).

M019S directly binds to recombinant Bax protein

We examined whether CSMs (M109S and M41S) directly bind Bax using a recombinant Bax protein (Figures 5E and S5). Binding was examined by the microscale thermophoresis (MST) assay.[26] M109S showed Bax-binding activity with the average K_d of 153.75 ± 55.8 nM calculated from four independent MST assay results. Figure 5E shows an example of MST assay detecting the biding of M109S and Bax (Kd = 178nM). Dexamethasone is a steroid hormone analog that has been shown to inhibit fibroblast cell death,[27,28] but it is not expected to bind Bax. Dexamethasone was used as a negative control, and the binding of Dexamethasone and Bax was not detected (Figure 5F).

M109S decreases mitochondrial oxygen consumption and reactive oxygen species, whereas M109S increases glycolysis

We noticed that the color of the culture medium of M109S-treated cells turned from red to orange a little bit faster than that of vehicle control, suggesting that the medium acidification was stimulated by M109S. Because lactate accumulation as a result of glycolysis is the common reason for medium acidification in cell culture, we speculated that M109S has an activity influencing cellular metabolism. To determine the effects of M109S on cellular metabolism, oxygen consumption rate (OCR) and extracellular acidification rate (ECAR) were measured using the Seahorse instrument. OCR and ECAR are the indicators of mitochondrial oxidative phosphorylation (OXPHOS) and glycolysis, respectively. At 1 μM concentration in MEF cell culture, M109S decreased maximal OCR (Figures 6E and 6F) and increased ECAR (Figures 6G and 6H). Interestingly, these effects were observed in both *Wt* and *bax*$^{-/-}$*bak*$^{-/-}$ (Bax/Bak double-knockout [DKO]) MEFs. A high dose of M109S (1 μM) also showed a slight suppression of the basal OCR and OCR for ATP production of *Wt* MEF (Figures 6A and 6C), but the effects were not statistically significant in *bax*$^{-/-}$*bak*$^{-/-}$ MEFs (Figures 6B and 6D).

Previous studies showed that OXPHOS inhibitors have neuroprotective activities by decreasing reactive oxygen species (ROS) generation from mitochondria.[29–32] Therefore, the effects of M109S on ROS were examined. As shown in Figures 6I and 6J, M109S decreased ROS levels both in *Wt* and *bax*$^{-/-}$*bak*$^{-/-}$ MEFs. N-acetyl cysteine (NAC) is known to reduce ROS levels in cells.[33] The effects of M109S (0.1–1 μM) on the ROS level in cultured MEFs were very similar to the effects of NAC (10–20 μM) (Figure 6I). Because the changes in the metabolism can impact the speed of cell division, we examined the effects of M109S on population doublings of cultured cells. M109S slightly decreased the speed of the population-doubling time of cultured MEFs (Figures 6K and 6L). The effect was more evident in *bax*$^{-/-}$*bak*$^{-/-}$ MEFs than in *Wt* MEFs. Probably M109S's effects on cell division speed become more detectable in *bax*$^{-/-}$*bak*$^{-/-}$ MEFs because the population doubling speed of *bax*$^{-/-}$*bak*$^{-/-}$ MEFs is faster than that of *Wt* MEFs. Altogether, these results indicate that independently of Bax inhibiting effect, M109S decreases the rate of oxygen consumption, which diminishes the levels of ROS in the cell. These different activities of M109S have likely additive protective effects against mitochondria-dependent cell death pathways. Especially in *in vivo* experiments, for example, in the case of the bright-light-induced retinopathy tested in Figure 3, the suppression of ROS may have an impact on cell protection from pathological damages.

DISCUSSION

We developed CSMs by utilizing a cell-based functional assay system that was developed to identify Bax inhibitors. The chemical structures of these CSMs are distinct from previously reported Bax inhibitors[12–14,34] that were identified through *in vitro* Bax binding and pore-forming assays. Through a medicinal chemistry program, M109S was developed as a lead compound that possesses cell protecting activities both *in vitro* and *in vivo*. M109S suppressed ABT-737-induced apoptosis in both Bax-only and Bak-only MEFs (Figure 4C). These observations suggest that M109S can inhibit apoptosis induced by Bax and Bak expressed at endogenous levels in the cell. M109S also inhibited apoptosis in STS-treated MEFs, obatoclax-treated ARPE19 cells, and etoposide-treated Neuro2a cells (Figures 4A–4I). However, M109S did not inhibit etoposide-induced apoptosis in HeLa cells (Figure 4G), suggesting that M109S is not a universal cell death inhibitor. Etoposide induces a certain level of cell death even in the absence of Bax and Bak.[22,23] In the case of HeLa cells, etoposide possibly activated the Bax-/Bak-independent pathway inducing apoptosis that cannot be inhibited by M109S. In the case of BAI-1, a previously reported Bax-inhibiting compound, it was shown that BAI-1 was not able to inhibit Bax-induced apoptosis of the cancer cells due to the abnormally high levels of Bax expression in the cancer cells.[34] Similar to BAI-1, M109S may show selective protection against cell death depending on the expression levels of Bax and other apoptosis-regulating proteins.

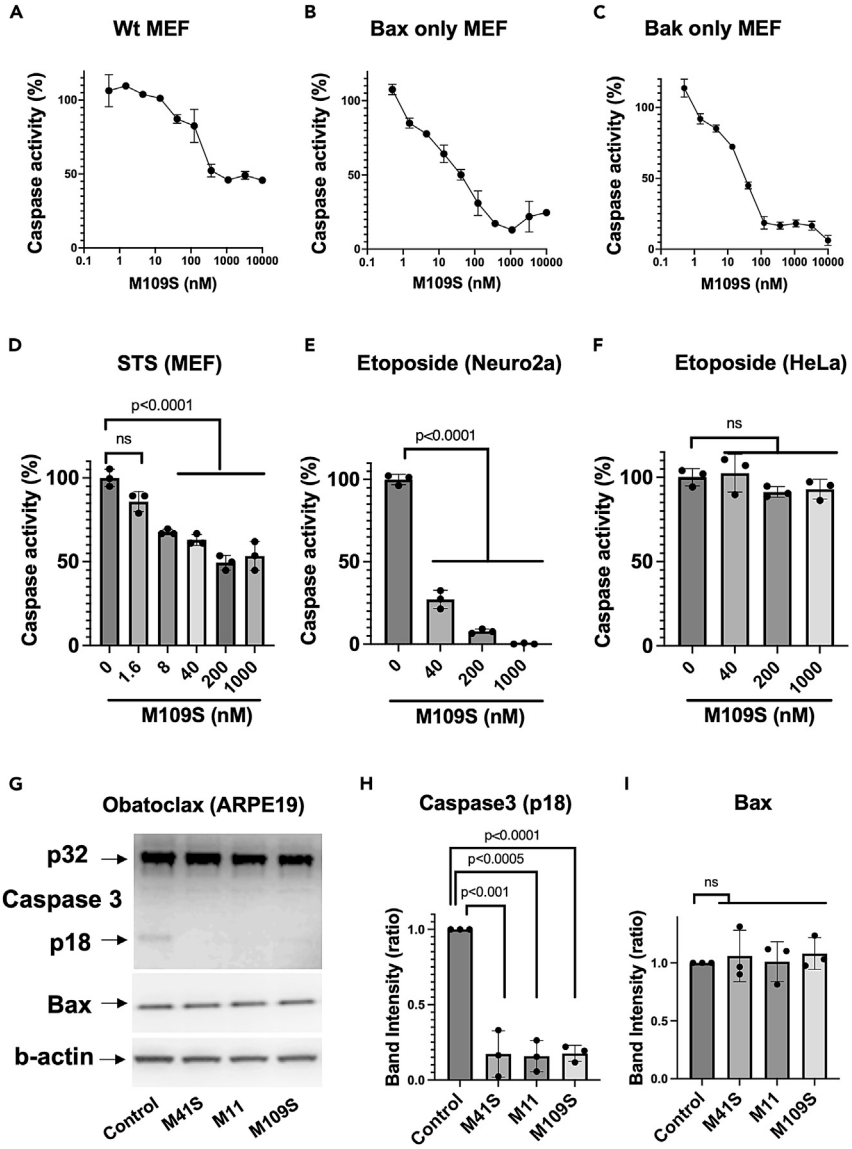

Figure 4. Effects of M109S on drug-induced apoptosis in cell culture

(A–C) M109S suppressed apoptosis induced by ABT-737 in wild-type (A), Bax-only ($bax^{+/+}bak^{-/-}$) (B), and Bak-only ($bax^{-/-}bak^{+/+}$) (C) MEFs. MEFs were cultured with ABT-737 (1 μM) with various doses of M109S for 24 h (WT and Bax-only) or 48 h (Bak-only). Caspase activity of vehicle control (ABT-737 and vehicle) was designated as 100%.

(D) M109S suppressed staurosporine (STS)-induced apoptosis in MEFs. MEFs were treated with STS (1 μM) for 4 h in the presence of various concentrations of M109S as indicated in the graph. M109S suppressed STS-induced caspase activation in a dose-dependent manner. The result of the statistical analysis (one-way ANOVA) is shown in each graph. "ns": no statistically significant difference was detected ($p > 0.05$).

(E) M109S inhibited etoposide-induced apoptosis in Neuro2a cells. Neuro2a cells were treated with etoposide (12.5 μM) for 24 h. Then, the medium was changed, and cells were incubated with various concentrations of M109S for an additional 24 h without etoposide. M109S suppressed etoposide-induced caspase activation. The result of the statistical analysis (one-way ANOVA) is shown. "ns": no statistically significant difference was detected ($p > 0.05$).

(F) M109S was not able to inhibit etoposide-induced apoptosis in HeLa cells. HeLa cells were treated with etoposide (12.5 μM) for 24 h. Then, the medium was changed, and cells were incubated with various concentrations of M109S for an additional 24 h without etoposide. M109S did not show significant inhibition of etoposide-induced caspase activation in HeLa cells. The graph shows the results of 12.5 μM etoposide. The result of the statistical analysis (one-way ANOVA) is shown. "ns": no statistically significant difference was detected ($p > 0.05$).

(G–I) M109S inhibited obatoclax-induced apoptosis in ARPE19 cells. AREP19 cells were incubated with obatoclax (100 nM) in the presence of 500 nM CSMs (M41S, M11, and M109S) for 24 h. Then, cells were collected and Western blot analyses of Caspase-3 and Bax were performed. CSMs suppressed obatoclax-induced Caspase activation (p18 fragment production by the cleavage of Caspase-3) (G and H). Bax expression was not affected by CSMs (I) (actin levels were used as loading control). The result of the Student's t test analysis is shown in each graph. "ns": no statistically significant difference was detected ($p > 0.05$). Data are presented as mean ± SD.

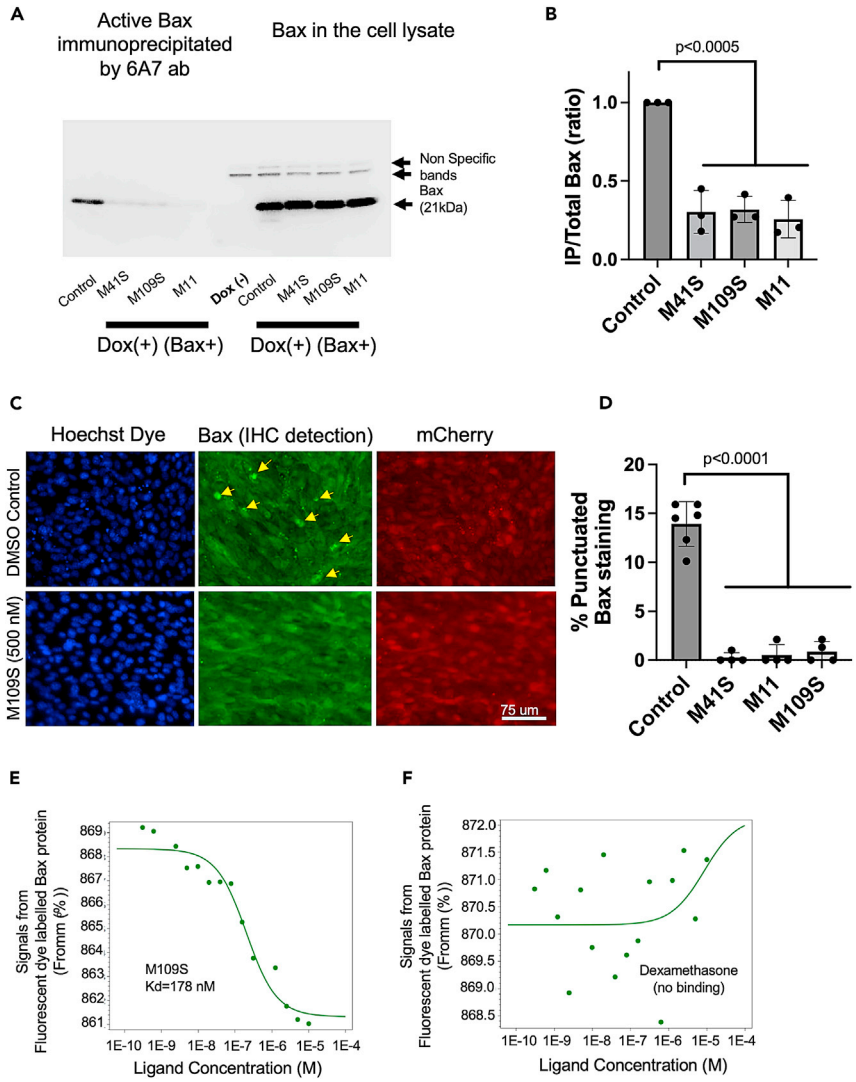

Figure 5. M109S inhibits Bax activation

(A and B) CSMs suppressed the conformation change of Bax. The N-terminus exposure of Bax occurs at the early step of Bax activation. Activated (conformationally changed) Bax can be immunoprecipitated by the 6A7 monoclonal antibody recognizing the N-terminus of Bax. iBax cells were treated with Dox for 48 h in the presence or absence of CSMs (M41S [50 nM], M109S [500 nM], or M11 [500 nM]). Cells were lysed with CHAPS buffer, and the lysates were subjected to immunoprecipitation (ip). (A) Western blot of immunoprecipitated Bax by 6A7 antibody and total Bax in the cell lysates are shown. (B) The ratio of the Western blot intensity of immunoprecipitated Bax (IP) and total Bax (total) is shown. CSMs significantly suppressed the amount of immunoprecipitated Bax without a significant change in the total Bax expression. The result of the Student's t test statistical analysis is shown in each graph. "ns": no statistically significant difference was detected ($p > 0.05$).

(C and D) CSMs suppressed mitochondrial translocation of Bax. iBax cells were fixed at 36 h after Dox treatment. Bax was detected by an anti-Bax polyclonal antibody (green fluorescence). The activation of the Dox-inducible promoter was confirmed by the detection of mCherry by red fluorescence. In vehicle (DMSO) control, punctuated Bax staining patterns associated with mitochondrial translocation were detected (indicated by arrows). The frequency of the punctuated staining was significantly reduced by CSMs (M41S, M11, and M109S). (D) Quantitative analysis of (C) is shown. The result of the Students' t test statistical analysis is shown. "ns": no statistically significant difference was detected ($p > 0.05$).

(E and F) CSMs bind purified recombinant Bax proteins. The interactions of CSMs and Bax were examined by microscale thermophoresis (MST) assay using His-tagged Bax. Panel E shows a representative dose-dependent Bax binding signal curve of M109S. A similar binding assay was performed multiple times, and the average of K_d was 153.75 + 55.8 nM (n = 4). Panel F shows a negative control experiment. The binding of Bax and dexamethasone was not detected. Data are presented as mean ± SD.

M109S protected photoreceptor cells from the bright-light-induced apoptosis in two mouse models of light-induced retinal degeneration related to Stargardt disease and age-related macular degeneration.[17–19] Previous studies showed that Bax plays an essential role in photoreceptor death in these retina degeneration mouse models.[17–19] The photoreceptor protection by M109S confirms that M109S penetrates the

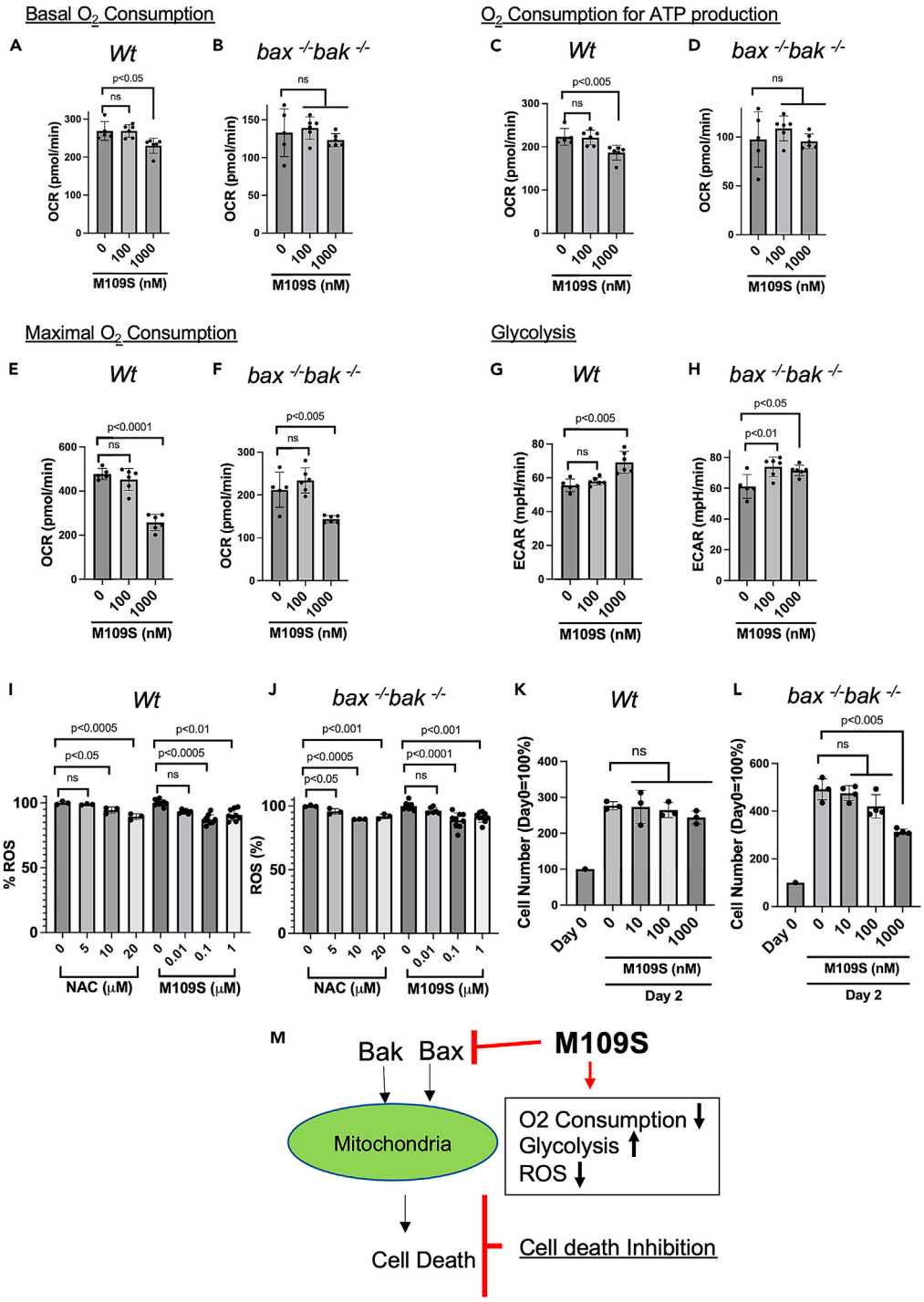

Figure 6. Effects of M109S on cellular metabolism

(A–H) M109S decreased the maximum oxygen consumption rate (OCR) and increased the extracellular acidification rate (ECAR) both in *Wt* and *bax*$^{-/-}$*bak*$^{-/-}$ MEFs. OCR and ECAR represent the activities of mitochondrial oxidative phosphorylation (OXPHOS) and glycolysis, respectively. The effect of M109S on metabolism was analyzed using the Seahorse mitochondria stress kit as described in STAR methods section. MEFs (*Wt* and *bax*$^{-/-}$*bak*$^{-/-}$) were incubated with or without M109s for 4 h before Seahorse analysis. M109S was also added to the culture medium during the Seahorse analysis procedure (approximately 3 h). (A–F) The levels of OCR of the basal (A and B), ATP production (C and D), and maximum oxygen consumption (E and F), are shown. (G and H) The basal ECAR is shown. M109S decreased maximal O_2 consumption and increased glycolysis in *Wt* and *bax*$^{-/-}$*bak*$^{-/-}$ MEFs. The result of the statistical analysis (one-way ANOVA) is shown in each graph. "ns": no statistically significant difference was detected ($p > 0.05$). Data are presented as mean ± SD.

Figure 6. *Continued*

(I and J) M109S decreases ROS levels in cell culture. ROS levels were measured by ROS-Glo-H_2O_2 assay kit (Promega). N-acetyl cysteine (NAC) or M109S was added to the culture medium for a total of 8 h (4 h before ROS substrate addition and 4 h during the incubation with ROS substrate). M109S addition decreased ROS levels both in *Wt* and $bax^{-/-}bak^{-/-}$ MEFs. The result of the statistical analysis (one-way ANOVA) is shown in each graph. "ns": no statistically significant difference was detected ($p > 0.05$). Data are presented as mean ± SD.

(K and L) A high dose of M109S (1 μM) slowed the cell division speed both in *Wt* and $bax^{-/-}bak^{-/-}$ MEFs. Forty thousand cells were plated in each well of 12 well plate (1 mL/well) on Day 0. The next day (24 h later), M109S was added to the medium, and cells were cultured for an additional 24 h, and the numbers of cells were counted. The cell number at Day 0 is designated 100%, and the ratio of cell number is shown. The result of the statistical analysis (one-way ANOVA) is shown in each graph. "ns": no statistically significant difference was detected ($p > 0.05$).

(M) Schematic explanation of the mechanism of action of CSMs. Data are presented as mean ± SD.

blood-retina barrier and functions as Bax inhibitor *in vivo*. Indeed, M109S was detected in the brain and retina in rats 24 h after oral administration (Figure 2G). Although further detailed toxicity studies are needed, the currently available data suggest that M109S may prevent the unwanted death of essential cells without significant side effects if it is used at therapeutic dose.

Bax-binding activity of CSMs was confirmed by the MST-binding assay. To be noted, the binding of CSMs to Bax was detected in NP40-containing buffer but not in CHAPS-containing buffer (Figure S5). It is known that NP40, but not CHAPS, induces a conformation change (N-terminus exposure) of Bax, which is one of the activation steps of Bax.[24,25] Therefore, the present data suggest that CSMs bind partially active Bax (the N-terminus exposed Bax). The Bax-binding character of CSMs is similar to that seen in anti-apoptotic Bcl-2 family proteins such as Bcl-2 and Bcl-XL.[24,25] For example, Bax binds Bcl-XL only in NP40-based buffer but not in CHAPS-containing (or detergent-free) buffer if cell lysates were prepared from healthy cells.[24] It is known that Bcl-XL, at the surface of the mitochondrial membrane, interacts with activated Bax (the N-terminus exposed Bax) and bounces Bax back to the cytosol.[35,36] As a result, Bcl-XL suppresses the mitochondrial translocation of Bax as well as the accumulation of active Bax in the cell, although the detailed mechanism of this process is not yet understood. Similar to Bcl-XL, CSMs attenuated the N-terminus exposure of Bax and suppressed mitochondrial translocation of Bax. CSMs and Bcl-XL may share a similar mechanism of action to suppress Bax-induced cell death. Further biochemical and structural biological studies are warranted to uncover the precise mechanism of action of Bax inhibition by CSMs.

We found that M109S affects metabolism in 2 ways: (1) by decreasing mitochondrial oxygen consumption and (2) by increasing glycolysis. It has been known that inhibitors of mitochondrial oxidative phosphorylation (OXPHOS) have activities rescuing cells from mitochondria-dependent cell death, especially in the case of ischemia-/reperfusion-induced cell death.[37–42] Furthermore, there is increasing evidence showing OXPHOS inhibitors protect neurons in mouse models of neurodegenerative diseases including Alzheimer and Parkinson diseases.[29–32] These neuroprotective effects of OXPHOS inhibitors have been explained by their activities decreasing ROS by suppressing mitochondrial oxygen consumption.[29–32] As shown in Figure 6, M109S decreased ROS in MEF cell culture. Therefore, in addition to the direct inhibition of Bax, the suppression of mitochondrial activities may contribute to the cell protection activity of M109S. However, these activities of M109S against mitochondrial activities and metabolism became evident at 1 μM concentration in the cell culture (Figure 6), which is approximately 40 times higher than M109S's EC_{50} (23.4 nM) of cell death inhibition (Figure 2). Therefore, the effects on mitochondrial activity may become important only when M109S is used at high dose. However, this finding suggests that we cannot neglect the possibility of side effects of M109S as an inhibitor of mitochondrial activity because the suppression of OXPHOS can cause energy deficiency when cells have high energy demand. In spite of the fact that M109S showed effects on metabolism both in *Wt* and $bax^{-/-}bak^{-/-}$ MEFs, we cannot completely exclude the possibility that the inhibition of Bax and Bak by M109S has a certain impact on mitochondrial function. Further careful investigation regarding the effects of M109S on mitochondria is warranted.

Although it is not directly related to the mechanism of action of M109S, we noticed that the basal OCR levels of Bax/Bak DKO MEF were lower than that of *Wt* MEFs (Figures 6A and 6B). This difference may suggest that Bax and Bak have influences on mitochondrial OCR. However, this difference may be due to the clonal difference because we experienced recording different OCR values among multiple clones derived from the same embryos. In the Figure S6, we show the effects of the transient expression of Bax or Bak in Bax/Bak DKO MEFs using iBax and iBak cells (Figure S6). The brief conclusion is that the expression of Bax or Bak (at the sublethal level, 24 h after the DOX-induced expression) did not show major impacts on OCR and ECAR of MEFs except a slight decrease of the basal OCR in Bak-expressed cells (Figure S6B). These results suggest that a transient expression of Bax and Bak does not significantly influence mitochondrial oxygen consumption and glycolysis at least in this experimental condition. Further careful studies are necessary to investigate Bax and Bak's role in mitochondrial function and glycolysis. M109S, iBax, and iBak may become useful research tools to investigate the influences of Bax and Bak on mitochondrial function and other cellular metabolism.

In summary, we developed small compounds protecting cells from mitochondria-dependent cell death. The pharmacokinetics of M109S is ideal for *in vivo* treatment. Importantly, orally administered M109S reached both the brain and retina, indicating that M109S penetrates the blood-brain/blood-retina barrier. Bax-mediated and mitochondria-initiated cell death are involved in various types of degenerative diseases including neurodegenerative disorders and cardiovascular dysfunctions (reviewed in[1]). For example, the inhibition of Bax-mediated cell death is known to attenuate pathological conditions in animal models of Alzheimer disease,[43] Parkinson disease,[44] amyotrophic lateral sclerosis,[45–47] Huntington disease,[48] ischemia-reperfusion tissue injuries,[49–51] and glaucoma.[52–54] M109S and its derivatives have the potential to become an important therapeutic agent that can be used to prevent unwanted cell death in these pathological conditions. The investigation of the mechanism of action of CSMs may shed new light on the previously unknown cell death mechanisms controlled by Bax and Bak.

Limitation of the study

In the present study, we found that M109S prevented blindness of mouse models of Stargardt disease and macular degeneration. However, these protective effects in mouse disease models do not guarantee that M109S can prevent blindness in human and other animals. We plan to extend our studies in other animals in the near future if fundings were obtained. In the present study, we used a selected group of cell lines (MEFs, Neruo2a, ARPE19, and HeLa cells) to investigate the mechanism of cell death inhibition by M109S. It is not yet certain whether the similar results can be seen in other cell lines. We plan to examine other types of primary cultured cells and cancer cell lines to further investigate the mechanism of action of M109S.

STAR★METHODS

Detailed methods are provided in the online version of this paper and include the following:

- KEY RESOURCES TABLE
- RESOURCE AVAILABILITY
  - Lead contact
  - Materials availability
  - Data and code availability
- EXPERIMENTAL MODEL AND STUDY PARTICIPANT DETAILS
  - Cell culture and generation of iRFP, iBax, and iBak cells
  - Animals care and treatment
- METHOD DETAILS
  - High-throughput screening of small compound library
  - Chemical synthesis and profiling tests
  - Western blot
  - Caspase measurement
  - Pharmacokinetic analysis
  - Retinal degeneration induced with bright light
  - Scanning laser ophthalmoscopy
  - SD-OCT
  - Retinal histology
  - Detection of rod and cone photoreceptors
  - 6A7 Ab bax immunoprecipitation
  - Bax immunocytochemistry
  - Microscale thermophoresis (MST)
  - Seahorse experiment
  - ROS measurement
  - Cell number measurement
- QUANTIFICATION AND STATISTICAL ANALYSIS
  - Statistical

SUPPLEMENTAL INFORMATION

Supplemental information can be found online at https://doi.org/10.1016/j.isci.2023.107916.

ACKNOWLEDGMENTS

Authors are grateful for invaluable advice and guidance by Dr. Diana Wetmore (Harrington Discovery Institute [HDI]) and Dr. Steven Brenner (HDI) throughout the project and for project management by Dr. Jeff Klein (HDI). We thank the past and present members of Matsuyama laboratory (Dr. James Palmer, Dr. Kelsey Jensen, David J WuWong, Sean Wang, Emma Heironimus, and Xiao-Yi Chen) for their assistance in plasmid production, cell image capture, and data analysis. We also thank Dr. David Wald for his advice on drug screening and the use of the Tet-ON system. This work was supported by Gund-Harrington Scholar Award (to SM) from Foundation Fighting Blindness and HDI; Department of Defense Vision Research Program W81XWH-20-1-0735 (to SM); National Institutes of Health (NIH) RO1-AG031903 (to SM); RO1 EY032874 (to BJ); RO1EY029169 (to JMG and MB); and P30 grants for Case Comprehensive Cancer Center (P30 CA043703) and Vision Science Research Center (P30 EY011373). Authors are grateful for the support to this project by Dr. Clark Distelhorst who was the leader of Cell Death research–related programs in Case Western Reserve University and Case Comprehensive Cancer Center.

AUTHOR CONTRIBUTIONS

Shigemi Matsuyama initiated the project and designed the experiments reported in Figures 1, 2, 4, 5, and 6. iRFP cells, iBax cells, and iBak cells as well as the CSM screening system were designed and generated by Shigemi Matsuyama. Mieko Matsuyama performed the experiments

together with Shigemi Matsuyama reported in Figures 1, 2 (except Figures 2E–2G), 4, 5, and 6. Jonah Scott-McKean analyzed the data of Figure 1F. Joseph Ortega and Beata Jastrzebska designed and performed the experiments reported in Figure 3. Yuri Fedorov and Drew Adams set up the high-throughput drug screening system with the Operetta system (Parkin Elmer), optimized the CSM screening system, and performed the screening. Jeannie Muller-Greven and Mathias Buck provide advice for the MST-binding assay and participated in the data analysis. William Greenlee performed the medicinal chemistry study during the entire project, and he designed all the CSMs. The first draft of the manuscript was prepared by Shigemi Matsuyama, and all the authors participated in editing the draft to complete the final version.

DECLARATION OF INTERESTS

SM and WG filed a patent application for the development of CSMs including M109S.[16] All other authors have no competing interest.

Received: March 17, 2023
Revised: July 27, 2023
Accepted: September 12, 2023
Published: September 17, 2023

REFERENCES

1. Singh, R., Letai, A., and Sarosiek, K. (2019). Regulation of apoptosis in health and disease: the balancing act of BCL-2 family proteins. Nat. Rev. Mol. Cell Biol. *20*, 175–193. https://doi.org/10.1038/s41580-018-0089-8.
2. Wei, M.C., Zong, W.X., Cheng, E.H., Lindsten, T., Panoutsakopoulou, V., Ross, A.J., Roth, K.A., MacGregor, G.R., Thompson, C.B., and Korsmeyer, S.J. (2001). Proapoptotic BAX and BAK: a requisite gateway to mitochondrial dysfunction and death. Science *292*, 727–730.
3. Walensky, L.D. (2019). Targeting BAX to drug death directly. Nat. Chem. Biol. *15*, 657–665. https://doi.org/10.1038/s41589-019-0306-6.
4. Pogmore, J.P., Uehling, D., and Andrews, D.W. (2021). Pharmacological Targeting of Executioner Proteins: Controlling Life and Death. J. Med. Chem. *64*, 5276–5290. https://doi.org/10.1021/acs.jmedchem.0c02200.
5. Spitz, A.Z., and Gavathiotis, E. (2022). Physiological and pharmacological modulation of BAX. Trends Pharmacol. Sci. *43*, 206–220. https://doi.org/10.1016/j.tips.2021.11.001.
6. Diepstraten, S.T., Anderson, M.A., Czabotar, P.E., Lessene, G., Strasser, A., and Kelly, G.L. (2022). The manipulation of apoptosis for cancer therapy using BH3-mimetic drugs. Nat. Rev. Cancer *22*, 45–64. https://doi.org/10.1038/s41568-021-00407-4.
7. Jensen, K., WuWong, D.J., Wong, S., Matsuyama, M., and Matsuyama, S. (2019). Pharmacological inhibition of Bax-induced cell death: Bax-inhibiting peptides and small compounds inhibiting Bax. Exp. Biol. Med. *244*, 621–629. https://doi.org/10.1177/1535370219833624.
8. Oltersdorf, T., Elmore, S.W., Shoemaker, A.R., Armstrong, R.C., Augeri, D.J., Belli, B.A., Bruncko, M., Deckwerth, T.L., Dinges, J., Hajduk, P.J., et al. (2005). An inhibitor of Bcl-2 family proteins induces regression of solid tumours. Nature *435*, 677–681. https://doi.org/10.1038/nature03579.
9. Ashkenazi, A., Fairbrother, W.J., Leverson, J.D., and Souers, A.J. (2017). From basic apoptosis discoveries to advanced selective BCL-2 family inhibitors. Nat. Rev. Drug Discov. *16*, 273–284. https://doi.org/10.1038/nrd.2016.253.
10. Bombrun, A., Gerber, P., Casi, G., Terradillos, O., Antonsson, B., and Halazy, S. (2003). 3,6-dibromocarbazole piperazine derivatives of 2-propanol as first inhibitors of cytochrome c release via Bax channel modulation. J. Med. Chem. *46*, 4365–4368. https://doi.org/10.1021/jm034107j.
11. Peixoto, P.M., Ryu, S.Y., Bombrun, A., Antonsson, B., and Kinnally, K.W. (2009). MAC inhibitors suppress mitochondrial apoptosis. Biochem. J. *423*, 381–387. https://doi.org/10.1042/BJ20090664.
12. Niu, X., Brahmbhatt, H., Mergenthaler, P., Zhang, Z., Sang, J., Daude, M., Ehlert, F.G.R., Diederich, W.E., Wong, E., Zhu, W., et al. (2017). A Small-Molecule Inhibitor of Bax and Bak Oligomerization Prevents Genotoxic Cell Death and Promotes Neuroprotection. Cell Chem. Biol. *24*, 493–506.e5. https://doi.org/10.1016/j.chembiol.2017.03.011.
13. Garner, T.P., Amgalan, D., Reyna, D.E., Li, S., Kitsis, R.N., and Gavathiotis, E. (2019). Small-molecule allosteric inhibitors of BAX. Nat. Chem. Biol. *15*, 322–330. https://doi.org/10.1038/s41589-018-0223-0.
14. Spitz, A.Z., Zacharioudakis, E., Reyna, D.E., Garner, T.P., and Gavathiotis, E. (2021). Eltrombopag directly inhibits BAX and prevents cell death. Nat. Commun. *12*, 1134. https://doi.org/10.1038/s41467-021-21224-1.
15. Loew, R., Heinz, N., Hampf, M., Bujard, H., and Gossen, M. (2010). Improved Tet-responsive promoters with minimized background expression. BMC Biotechnol. *10*, 81. https://doi.org/10.1186/1472-6750-10-81.
16. Matsuyama, S., and Greenlee, W. (2020). The Use of Novel Small Compounds of Bax Inhibitors to Protect Damaged Cells from Death (US Patent Office). https://patents.google.com/patent/WO2021002986A2/en.
17. Sawada, O., Perusek, L., Kohno, H., Howell, S.J., Maeda, A., Matsuyama, S., and Maeda, T. (2014). All-trans-retinal induces Bax activation via DNA damage to mediate retinal cell apoptosis. Exp. Eye Res. *123*, 27–36. https://doi.org/10.1016/j.exer.2014.04.003.
18. Maeda, A., Maeda, T., Golczak, M., Chou, S., Desai, A., Hoppel, C.L., Matsuyama, S., and Palczewski, K. (2009). Involvement of all-trans-retinal in acute light-induced retinopathy of mice. J. Biol. Chem. *284*, 15173–15183. https://doi.org/10.1074/jbc.M900322200.
19. Ortega, J.T., Parmar, T., Golczak, M., and Jastrzebska, B. (2021). Protective Effects of Flavonoids in Acute Models of Light-Induced Retinal Degeneration. Mol. Pharmacol. *99*, 60–77. https://doi.org/10.1124/molpharm.120.000072.
20. Certo, M., Del Gaizo Moore, V., Nishino, M., Wei, G., Korsmeyer, S., Armstrong, S.A., and Letai, A. (2006). Mitochondria primed by death signals determine cellular addiction to antiapoptotic BCL-2 family members. Cancer Cell *9*, 351–365. https://doi.org/10.1016/j.ccr.2006.03.027.
21. Vogler, M., Weber, K., Dinsdale, D., Schmitz, I., Schulze-Osthoff, K., Dyer, M.J.S., and Cohen, G.M. (2009). Different forms of cell death induced by putative BCL2 inhibitors. Cell Death Differ. *16*, 1030–1039. https://doi.org/10.1038/cdd.2009.48.
22. Tu, H.C., Ren, D., Wang, G.X., Chen, D.Y., Westergard, T.D., Kim, H., Sasagawa, S., Hsieh, J.J.D., and Cheng, E.H.Y. (2009). The p53-cathepsin axis cooperates with ROS to activate programmed necrotic death upon DNA damage. Proc. Natl. Acad. Sci. USA. *106*, 1093–1098. https://doi.org/10.1073/pnas.0808173106.
23. Han, Y., Qu, Y.Q., Mok, S.W.F., Chen, J., Xia, C.L., He, H.Q., Li, Z., Zhang, W., Qiu, C.L., Liu, L., et al. (2019). A Novel Drug Resistance Mechanism: Genetic Loss of Xeroderma Pigmentosum Complementation Group C (XPC) Enhances Glycolysis-Mediated Drug Resistance in DLD-1 Colon Cancer Cells. Front. Pharmacol. *10*, 912. https://doi.org/10.3389/fphar.2019.00912.
24. Hsu, Y.T., and Youle, R.J. (1998). Bax in murine thymus is a soluble monomeric protein that displays differential detergent-induced conformations. J. Biol. Chem. *273*, 10777–10783.
25. Nechushtan, A., Smith, C.L., Hsu, Y.T., and Youle, R.J. (1999). Conformation of the Bax C-terminus regulates subcellular location and cell death. Embo J. *18*, 2330–2341.
26. Wienken, C.J., Baaske, P., Rothbauer, U., Braun, D., and Duhr, S. (2010). Protein-binding assays in biological liquids using microscale thermophoresis. Nat. Commun. *1*, 100. https://doi.org/10.1038/ncomms1093.
27. Gascoyne, D.M., Kypta, R.M., and Vivanco, M.d.M. (2003). Glucocorticoids inhibit apoptosis during fibrosarcoma development by transcriptionally activating Bcl-xL. J. Biol. Chem. *278*, 18022–18029. https://doi.org/10.1074/jbc.M301812200.
28. Amsterdam, A., Tajima, K., and Sasson, R. (2002). Cell-specific regulation of apoptosis by glucocorticoids: implication to their anti-inflammatory action. Biochem. Pharmacol.

64, 843–850. https://doi.org/10.1016/s0006-2952(02)01147-4.

29. Procaccio, V., Bris, C., Chao de la Barca, J.M., Oca, F., Chevrollier, A., Amati-Bonneau, P., Bonneau, D., and Reynier, P. (2014). Perspectives of drug-based neuroprotection targeting mitochondria. Rev. Neurol. *170*, 390–400. https://doi.org/10.1016/j.neurol.2014.03.005.
30. Cunnane, S.C., Trushina, E., Morland, C., Prigione, A., Casadesus, G., Andrews, Z.B., Beal, M.F., Bergersen, L.H., Brinton, R.D., de la Monte, S., et al. (2020). Brain energy rescue: an emerging therapeutic concept for neurodegenerative disorders of ageing. Nat. Rev. Drug Discov. *19*, 609–633. https://doi.org/10.1038/s41573-020-0072-x.
31. Stojakovic, A., Trushin, S., Sheu, A., Khalili, L., Chang, S.Y., Li, X., Christensen, T., Salisbury, J.L., Geroux, R.E., Gateno, B., et al. (2021). Partial inhibition of mitochondrial complex I ameliorates Alzheimer's disease pathology and cognition in APP/PS1 female mice. Commun. Biol. *4*, 61. https://doi.org/10.1038/s42003-020-01584-y.
32. Gao, H., Tripathi, U., Trushin, S., Okromelidze, L., Pichurin, N.P., Wei, L., Zhuang, Y., Wang, L., and Trushina, E. (2021). A genome-wide association study in human lymphoblastoid cells supports safety of mitochondrial complex I inhibitor. Mitochondrion *58*, 83–94. https://doi.org/10.1016/j.mito.2021.02.005.
33. Ezerina, D., Takano, Y., Hanaoka, K., Urano, Y., and Dick, T.P. (2018). N-Acetyl Cysteine Functions as a Fast-Acting Antioxidant by Triggering Intracellular H2S and Sulfane Sulfur Production. Cell Chem. Biol. *25*, 447–459.e4. https://doi.org/10.1016/j.chembiol.2018.01.011.
34. Amgalan, D., Garner, T.P., Pekson, R., Jia, X.F., Yanamandala, M., Paulino, V., Liang, F.G., Corbalan, J.J., Lee, J., Chen, Y., et al. (2020). A small-molecule allosteric inhibitor of BAX protects against doxorubicin-induced cardiomyopathy. Nat. Cancer *1*, 315–328. https://doi.org/10.1038/s43018-020-0039-1.
35. Edlich, F., Banerjee, S., Suzuki, M., Cleland, M.M., Arnoult, D., Wang, C., Neutzner, A., Tjandra, N., and Youle, R.J. (2011). Bcl-x(L) retrotranslocates Bax from the mitochondria into the cytosol. Cell *145*, 104–116. https://doi.org/10.1016/j.cell.2011.02.034.
36. Todt, F., Cakir, Z., Reichenbach, F., Youle, R.J., and Edlich, F. (2013). The C-terminal helix of Bcl-x(L) mediates Bax retrotranslocation from the mitochondria. Cell Death Differ. *20*, 333–342. https://doi.org/10.1038/cdd.2012.131.
37. Gohil, V.M., Sheth, S.A., Nilsson, R., Wojtovich, A.P., Lee, J.H., Perocchi, F., Chen, W., Clish, C.B., Ayata, C., Brookes, P.S., and Mootha, V.K. (2010). Nutrient-sensitized screening for drugs that shift energy metabolism from mitochondrial respiration to glycolysis. Nat. Biotechnol. *28*, 249–255. https://doi.org/10.1038/nbt.1606.
38. Morciano, G., Preti, D., Pedriali, G., Aquila, G., Missiroli, S., Fantinati, A., Caroccia, N., Pacifico, S., Bonora, M., Talarico, A., et al. (2018). Discovery of Novel 1,3,8-Triazaspiro [4.5]decane Derivatives That Target the c Subunit of F1/FO-Adenosine Triphosphate (ATP) Synthase for the Treatment of Reperfusion Damage in Myocardial Infarction. J. Med. Chem. *61*, 7131–7143. https://doi.org/10.1021/acs.jmedchem.8b00278.
39. Hong, S., and Pedersen, P.L. (2008). ATP synthase and the actions of inhibitors utilized to study its roles in human health, disease, and other scientific areas. Microbiol. Mol. Biol. Rev. *72*, 590–641. Table of Contents. https://doi.org/10.1128/MMBR.00016-08.
40. Johnson, J.A., and Ogbi, M. (2011). Targeting the F1Fo ATP Synthase: modulation of the body's powerhouse and its implications for human disease. Curr. Med. Chem. *18*, 4684–4714. https://doi.org/10.2174/092986711797379177.
41. Grover, G.J., and Malm, J. (2008). Pharmacological profile of the selective mitochondrial F1F0 ATP hydrolase inhibitor BMS-199264 in myocardial ischemia. Cardiovasc. Ther. *26*, 287–296. https://doi.org/10.1111/j.1755-5922.2008.00065.x.
42. Matsuyama, S., Xu, Q., Velours, J., and Reed, J.C. (1998). The Mitochondrial F0F1-ATPase proton pump is required for function of the proapoptotic protein Bax in yeast and mammalian cells. Mol. Cell *1*, 327–336.
43. Rohn, T.T., Vyas, V., Hernandez-Estrada, T., Nichol, K.E., Christie, L.A., and Head, E. (2008). Lack of pathology in a triple transgenic mouse model of Alzheimer's disease after overexpression of the anti-apoptotic protein Bcl-2. J. Neurosci. *28*, 3051–3059. https://doi.org/10.1523/JNEUROSCI.5620-07.2008.
44. Perier, C., Bové, J., Wu, D.C., Dehay, B., Choi, D.K., Jackson-Lewis, V., Rathke-Hartlieb, S., Bouillet, P., Strasser, A., Schulz, J.B., et al. (2007). Two molecular pathways initiate mitochondria-dependent dopaminergic neurodegeneration in experimental Parkinson's disease. Proc. Natl. Acad. Sci. USA *104*, 8161–8166. https://doi.org/10.1073/pnas.0609874104.
45. Gould, T.W., Buss, R.R., Vinsant, S., Prevette, D., Sun, W., Knudson, C.M., Milligan, C.E., and Oppenheim, R.W. (2006). Complete dissociation of motor neuron death from motor dysfunction by Bax deletion in a mouse model of ALS. J. Neurosci. *26*, 8774–8786. https://doi.org/10.1523/JNEUROSCI.2315-06.2006.
46. Steele, A.D., and Yi, C.H. (2006). Neuromuscular denervation: Bax up against the wall in amyotrophic lateral sclerosis. J. Neurosci. *26*, 12849–12851. https://doi.org/10.1523/jneurosci.4086-06.2006.
47. Reyes, N.A., Fisher, J.K., Austgen, K., VandenBerg, S., Huang, E.J., and Oakes, S.A. (2010). Blocking the mitochondrial apoptotic pathway preserves motor neuron viability and function in a mouse model of amyotrophic lateral sclerosis. J. Clin. Invest. *120*, 3673–3679. https://doi.org/10.1172/JCI42986.
48. Hickey, M.A., and Chesselet, M.F. (2003). Apoptosis in Huntington's disease. Prog. Neuro-Psychopharmacol. Biol. Psychiatry *27*, 255–265. https://doi.org/10.1016/S0278-5846(03)00021-6.
49. Gibson, M.E., Han, B.H., Choi, J., Knudson, C.M., Korsmeyer, S.J., Parsadanian, M., and Holtzman, D.M. (2001). BAX contributes to apoptotic-like death following neonatal hypoxia-ischemia: evidence for distinct apoptosis pathways. Mol. Med. *7*, 644–655.
50. Zhang, X., Chen, Y., Jenkins, L.W., Kochanek, P.M., and Clark, R.S.B. (2005). Bench-to-bedside review: Apoptosis/programmed cell death triggered by traumatic brain injury. Crit. Care *9*, 66–75. https://doi.org/10.1186/cc2950.
51. Raghupathi, R., Graham, D.I., and McIntosh, T.K. (2000). Apoptosis after traumatic brain injury. J. Neurotrauma *17*, 927–938. https://doi.org/10.1089/neu.2000.17.927.
52. Maes, M.E., Schlamp, C.L., and Nickells, R.W. (2017). BAX to basics: How the BCL2 gene family controls the death of retinal ganglion cells. Prog. Retin. Eye Res. *57*, 1–25. https://doi.org/10.1016/j.preteyeres.2017.01.002.
53. Donahue, R.J., Maes, M.E., Grosser, J.A., and Nickells, R.W. (2020). BAX-Depleted Retinal Ganglion Cells Survive and Become Quiescent Following Optic Nerve Damage. Mol. Neurobiol. *57*, 1070–1084. https://doi.org/10.1007/s12035-019-01783-7.
54. Donahue, R.J., Fehrman, R.L., Gustafson, J.R., and Nickells, R.W. (2021). BCLX(L) gene therapy moderates neuropathology in the DBA/2J mouse model of inherited glaucoma. Cell Death Dis. *12*, 781. https://doi.org/10.1038/s41419-021-04068-x.
55. Maeda, A., Maeda, T., Golczak, M., and Palczewski, K. (2008). Retinopathy in mice induced by disrupted all-trans-retinal clearance. J. Biol. Chem. *283*, 26684–26693. https://doi.org/10.1074/jbc.M804505200.
56. Gao, S., Parmar, T., Palczewska, G., Dong, Z., Golczak, M., Palczewski, K., and Jastrzebska, B. (2018). Protective Effect of a Locked Retinal Chromophore Analog against Light-Induced Retinal Degeneration. Mol. Pharmacol. *94*, 1132–1144. https://doi.org/10.1124/mol.118.112581.
57. Kim, S.R., Fishkin, N., Kong, J., Nakanishi, K., Allikmets, R., and Sparrow, J.R. (2004). Rpe65 Leu450Met variant is associated with reduced levels of the retinal pigment epithelium lipofuscin fluorophores A2E and iso-A2E. Proc. Natl. Acad. Sci. USA *101*, 11668–11672. https://doi.org/10.1073/pnas.0403499101.
58. Chen, Y., Okano, K., Maeda, T., Chauhan, V., Golczak, M., Maeda, A., and Palczewski, K. (2012). Mechanism of all-trans-retinal toxicity with implications for stargardt disease and age-related macular degeneration. J. Biol. Chem. *287*, 5059–5069. https://doi.org/10.1074/jbc.M111.315432.
59. Gama, V., Gomez, J.A., Mayo, L.D., Jackson, M.W., Danielpour, D., Song, K., Haas, A.L., Laughlin, M.J., and Matsuyama, S. (2009). Hdm2 is a ubiquitin ligase of Ku70-Akt promotes cell survival by inhibiting Hdm2-dependent Ku70 destabilization. Cell Death Differ. *16*, 758–769. https://doi.org/10.1038/cdd.2009.6.

STAR★METHODS

KEY RESOURCES TABLE

REAGENT or RESOURCE	SOURCE	IDENTIFIER
Antibodies		
anti-Bax polyclonal antibody	ProteinTech	Cat# 50599-2-IG; RRID: AB_2061561
anti-Bax Rabbit Polyclonal antibody	BD Pharmingen	Cat# BD 554104; RRID: AB_395241
Agarose beads conjugated with anti-Bax monoclonal antibody (clone 6A7)	Santa Cruz	Cat# sc-23959AC;RRID: AB_626728
anti-Bak	Santa Cruz	Cat# sc-832; RRID: AB_2063265
anti-Bcl-XL	Santa Cruz	Cat# sc-1690; RRID: AB_630918
anti-Caspase-3	Cell Signaling	Cat#9662s; RRID: AB_331439
anti-beta actin	Sigma-Aldrich	Cat#A5441; RRID: AB_476744
Anti-rabbit IgG-HRP	Kindle Bioscience	Cat# R1006; RRID: AB_2800464
Anti-mouse IgG-HRP	Kindle Bioscience	Cat#R1005; RRID: AB_2800463
Goat-*anti*-Mouse IgG (H + L)	ThermoFisher Scientific	Cat# G-21040; RRID: AB_2536527
Critical commercial assays		
Capsase-Glo 3/7 Assay kit	Promega	G8093
ROS-Glo-H_2O_2 Assay kit	Promega	G8820
His-Tag labeling Kit RED-tris-NTA 2^{ND} generation	Nanotemper	MO-L018
XF Cell Mito Stress test kit	Agilent	103015–100
Deposited data		
The data for all the graphs in this article.	Mendeley Data	https://doi.org/10.17632/tsdd5gmzcw.1
Experimental models: Cell lines		
iWT (wild type MEF, C57BL6 from The Jackson Lab)	This study	
iBBKO (Bax Bak doublr KO MEFs	This study	
iRFP (mCherry inducible iBBKO)	This study	
iBax (Bax inducible iBBKO)	This study	
iBak (Bak inducible iBBKO)	This study	
HeLa	ATCC	CRM-CCL-2
Neuro2a	ATCC	CCL-131
ARPE19	ATCC	CRL-2302
Experimental models: Organisms/strains		
Balb/c mouse	Jackson Lab	000651
Abc4−/−Rdh8−/− mouse	Jackson Lab	030503
Recombinant DNA		
pLVX-EF1a-TET3G	Takarabio	631359
pLVX-TRE3G-mCehrry	Takarabio	631360
Software and algorithms		
Prism	Dotmatics Graphpad	https://www.graphpad.com/scientific-software/prism/

(*Continued on next page*)

Continued

REAGENT or RESOURCE	SOURCE	IDENTIFIER
Other		
DMEM	ThermoFisher	11995
Fetal Calf Serum	Fisher Scientific	12999102
Doxycycline Hyclate	SigmaAldrich	33429-100MG-R
Puromycin	Dot scientific	DSP33020–0.025
Geneticin (G418)	ThermoFisher Scientific	10131027
Penicillin/Streptomycin	Fisher	SV30010
(2-Hydroxypropyl)-beta-cyclodexitrin (bCD)	Sigma-Aldrich	332607
Etoposide	Sigma-Aldrich	E1383
ABT-737	Sellekchem	S1002
Obatoclax	Cayman Chemical	11499
Staurosporine	Sigma-Aldrich	No. S6942
Dexamethasone	Sigma-Aldrich	D4902
M5 (R, S)	This study	
M6 (R, S)	This study	
M7 (R, S)	This study	
M11	This study	
M109S	This study	
Bax Channle Blocker	Tocris	No. 2160
iMac2	Tocris	No. 3749
Eltrombopag	Sigma-Aldrich	SML3182

RESOURCE AVAILABILITY

Lead contact

Further information and requests for resources and reagents should be directed to and will be fulfilled by the lead contact, Shigemi Matsuyama (shigemi.matsuyama@case.edu).

Materials availability

There are restrictions on the availability of all newly synthesized chemicals and cell lines used in this study due to potential requirements for materials transfer agreements with the host institution where these materials were generated.

Data and code availability

The data for all the graphs have been deposited at Mendeley Data (https://doi.org/10.17632/tsdd5gmzcw.1) and are publicly available as of the date of publication. Any additional information required to reanalyze the data reported in this paper is available upon request from the lead contact.

EXPERIMENTAL MODEL AND STUDY PARTICIPANT DETAILS

Cell culture and generation of iRFP, iBax, and iBak cells

Mouse embryonic fibroblasts (MEFs) from *Wt* and $bax^{-/-}bak^{-/-}$ mice (C57BL/6J background, generated by crossing $bax^{+/-}$ and $bak^{-/-}$ mice originally obtained from The Jackson Lab) were established in Matsuyama lab, and were immortalized by SV40LT expression. To introduce Tet-ON system (Tets-On inducible system, Takara, Madison, WI), a set of two plasmids were introduced to $bax^{-/-}bak^{-/-}$ MEFs to establish each cell line. The pLVX-EF1a-TET3G carrying Tet-inducible transcription factor was used for all three cell lines. pLVX-TRE3G-mCehrry (original plasmid with only mCherry), pLVX -TRE3G-mCherry carrying cDNAs of human Bax or human Bak, were introduced to generate cell lines of iRFP, iBax, and iBak respectively. These plasmids were introduced into the cells by using Lentivirus transfection system. Doxycycline (Dox) (100 ng/mL) was used to activate Tet-ON system to induce mCherry, Bax, and Bak. To maintain transfected genes, puromycin (1 μg/mL) sand G418 (750 μg/mL) were added to the MEF medium. The MEF medium is made from DMEM High Glucose (ThermoFisher Catlog Number11995) supplemented with 10% Fetal Calf Serum (FCS, Fisher Scientific Cat No.12999102), 2 mM (final concentration) Sodium Pyruvate,

6 mM L-Glutamine (Final concentration), 100U/mL (Penicillin-Streptomycin), and 1% of Non-Essential Amino Acid supplement (Gibco, 11140-050).

Animals care and treatment

Both male and female mice were used in all experiments. All mice were housed in the Animal Resource Center at the School of Medicine, Case Western Reserve University (CWRU), and maintained in a 12-h light/dark cycle. All mice were housed in individually ventilated cages with up to 5 mice per cage.

Double-knockout mice *Abca4*$^{-/-}$*Rdh8*$^{-/-}$ with 129Sv or C57BL/6 background that lacks ABCA4 transporter and retinol dehydrogenase 8 (RDH8)[55] at 5–6 weeks of age were used to evaluate the protective effect of a M109S on retinal degeneration induced by acute light. *Abca4*$^{-/-}$*Rdh8*$^{-/-}$ mice do not carry the *Rd8* mutation, however, they carry the Leu variation at amino acid 450 of retinal pigment epithelium 65 kDa protein (RPE65).[56,57] The substitution of Leu to Met in the *Rpe65* gene that exists in inbreed mice decreases sensitivity to retinal damage induced by bright light.[57] Balb/cJ (RRID:IMSR_JAX:000651) mice were used as WT control. All animal procedures and experimental protocols were approved by the Institutional Animal Care and Use Committee at CWRU and conformed to recommendations of both the American Veterinary Medical Association Panel on Euthanasia and the Association for Research in Vision and Ophthalmology.

METHOD DETAILS

High-throughput screening of small compound library

We used a 50,000 small compound library purchased from ChemBridge (San Diego, CA) to identify the compounds protecting cells from Bax-induced cell death using iBax cells (passage of iBax cells were used in the screening). 386 well plates and Operetta Image analysis system (PerkinElmer) were used for the screening. First, each compound was added together with Dox (100 ng/mL) to the culture media of iBax cells to the final concentration of 10 μM. Cells were cultured for 48 h and fixed by 2% paraformaldehyde (PFA) and the nuclei were stained with Hoechst 33258. Cell images were captured using both RFP and DAPI filter channels. RFP filter channel was used to monitor the mCherry expression. The compounds maintaining 80% and higher mCherry expression of the control cells (only Dox addition) were analyzed. DAPI filter channel was used to analyze the percentage (%) of cells with apoptotic nuclei (pyknosis). The best 50 chemicals were selected, and they were subjected to examine the dose-dependent effects to confirm the cytoprotective activities. After the best 50 hit compounds were selected, and two groups of chemicals were found Group 1 (M5 and M6 were the best Bax inhibitors in this group) and Group 2 (M7 was the best Bax inhibitor in this group)). We examined whether these 50 chemicals can also inhibit Bak-induced cell death in iBak cells. However, these compounds were not effective in inhibiting Bak-induced cell death in iBak cells.

Chemical synthesis and profiling tests

All the chemical synthesis were performed by Wuxi AppTech (Hong-Kong, China) based on the chemical design by Dr. William Greenlee. To select the lead compounds, the hit compounds were subjected to the profiling tests examining, kinetic solubility, Caco-2 cell permeability, microsomal stability (t ½ min), and plasma protein binding. These tests were performed by Wuxi AppPtech.

Western blot

To analyze the expression levels of Bcl-2 family proteins, Caspase-3, and beta-tubulin, cells were lysed in RIPA buffer and 20 μg of total protein was subjected to Western blot analysis using 4–20% gradient gel (Invitrogen). The primary antibodies used in this study are: anti-Bax antibody (Proteintech, 50599-2-IG, 5000X), anti-Bcl-2 antibody (SantaCruz, sc-7382, 500X), anti-Bc-XL antibody (SantaCruz, sc-1690, 500X), Caspase-3 (Cell Signaling, 9662, 1000X), and anti-beta actin (Sigma Aldrich, A5441, 20,000X). The secondary antibodies used for this study were anti-Rabbit-HRP (Kindle Biosciences, R1006, 1000X) and anti-mouse IgG-HRP (Kindle Biosciences, R1005, 1000X). Western blot signals were captured by Kwik Quant Imager (Kindle Biosciences), and the densitometric analysis was performed by ImageJ.

Caspase measurement

Promega's Capsase-Glo 3/7 Assay kit (G8093, Promega) was used to measure caspase activity according to the manufacturer's protocol. iBax and MEFs (ABT-737- and Staurosporine (STS)-induced apoptosis): iBax cells or MEFs were seeded at the density of 16,000 cells/100 μL/well (for ABT-737) or 20,000 cells/100 μL/well (for STS) in 96 well plates on Day 0. For culture medium, MEF medium was used. To determine the effects of CSMs on Caspase activation by Bax overexpression, Dox (100 ng/mL) and CSMs (various concentrations as indicated in the figures) were added to the culture media on Day 1. On Day 3, cells were subjected to Caspase assay. To examine the effects of CSMs against 1 μM ABT-737 (S1002, Sellekchem), cells were treated with ABT-737 together with various concentrations of CSMs. On Day 1 (*Wt* (passage 10) and Bax only (passage 11) cells) and Day 2 (Bak only cells (passage 10), Bak only cells die slower than wt and Bax-only cells)), Caspase activity was measured. To examine the effects of M109S against STS-induced apoptosis, MEFs were pre-incubated with M109S for 2 h before STS (1 μM) addition to the medium. Four hours after STS addition, Caspase assay buffer containing cell lysis reagent was added to each well, and cells were subjected to Caspase measurement. Neuro2a and HeLa cells (Etoposide-induced apoptosis: Cells were seeded at the density of 10,000 cells/100 μL/well in 96 well plates on Day 0. On day 1, etoposide (12.5 μM to Neuro2a (ATCC, passage 12), 12.5 or 25.0 μM or HeLa cells (ATCC, passage 11), respectively) were added to the culture media. On day 2, media were replaced with fresh media containing various concentrations of M109S without etoposide. On day 3, Caspase assay buffer was added to each well and Caspase activity was measured.

Pharmacokinetic analysis

The compounds were dissolved in 15% (2-Hydroxypropyl)-beta-cyclodexitrin (bCD) (and they were administered to the mice or rats by oral gavage, intrapreneurial (i.p.), or intravenous (i.v.) injection. At the time point of 0.5, 1, 2, 4, 8, and 24 h, the concentration in the blood plasma (3 mice for each time point) were measured by LC-MS/MS analysis. The concentrations in the retina and brain were also measured 24 h after the administration. These PK analyses of mice and rats were performed by Wuxi AppTech (Hong-Kong, China) and PharmOptima (Portage, Michigan), respectively.

Retinal degeneration induced with bright light

Twenty 4 h before the treatment, 4–5 weeks old *Abca4*$^{-/-}$*Rdh8*$^{-/-}$ mice and 6–8 weeks old Balb/cJ mice were dark-adapted. M109 was dissolved in the 15% 2-hydroxypropyl-β-cyclodextrin vehicle and administered to mice by oral gavage. *Abca4*$^{-/-}$*Rdh8*$^{-/-}$ mice were administered with M109S at 1, 2.5, 5, 10, and 20 mg/kg body weight (b.w.) 24 h and 2 h before the exposure to light, while Balb/cJ mice were gavaged with M109S at a dose of 20 mg/kg b.w. 2-hydroxypropyl-β-cyclodextrin vehicle was administered to control mice. To initiate the retinal damage, mice pupils were dilated with 1% tropicamide and *Abca4*$^{-/-}$*Rdh8*$^{-/-}$ mice were exposed to 10,000 lux white light for 30 min, delivered from a 150-W bulb (Hampton Bay; Home Depot, Atlanta, GA).[58] Balb/cJ mice were exposed to 12,000 lux light for 2 h. After illumination, mice were kept in the dark for 7 days. Treatment with M109 or vehicle was repeated 24 and 48 h after the exposure to light. The health of the retina was assessed *in vivo* by imaging using spectral domain optical coherence tomography (SD-OCT). Next, mice were euthanized and eyes were collected for histological evaluation. Six mice were used in each experimental group.

Scanning laser ophthalmoscopy

The Scanning Laser Ophthalmoscopy (SLO) (Heidelberg Engineering, Franklin, MA) was used to image the *in vivo* whole-fundus mouse retinas. *Abca4*$^{-/-}$*Rdh8*$^{-/-}$ mice were subjected to SLO imaging immediately after the acquired SD-OCT imaging. The number of autofluorescent spots (AF) detected in different experimental groups was quantified and compared to determine the statistical significance. Six mice were used in each experimental group.

SD-OCT

Ultrahigh-resolution SD-OCT (Bioptigen, Morrisville, NC) *in vivo* imaging was used to evaluate the effect of M109S treatment on retinal structure in *Abca4*$^{-/-}$*Rdh8*$^{-/-}$ mice subjected to bright light-induced retinal damage.[58] Before imaging, mice pupils were dilated with 1% tropicamide and anesthetized by i.p. injection of a cocktail containing ketamine (20 mg/mL) and xylazine (1.75 mg/mL) at a dose of 4 μL/g b.w. The a-scan/b-scan ratio was set at 1200 lines. The retinal images were obtained by scanning at 0 and 90° in the b-mode. Five image frames were captured and averaged. To determine the changes in the retinas of mice treated with M109S and exposed to bright light and control mice treated with vehicle or non-treated and dark-adapted mice were determined by measuring the outer nuclear layer (ONL) thickness at 0.15–0.75 mm from the optic nerve head (ONH). Values of the ONL thickness were plotted using means and standard deviation. For each experimental group, six mice were used.

Retinal histology

The effect of M109S on the retinal morphology in *Abca4*$^{-/-}$*Rdh8*$^{-/-}$ mice exposed to bright light was determined by retinal histology analysis. Eyes were collected from non-treated mice kept in the dark, treated with 15% 2-hydroxypropyl-β-cyclodextrin vehicle or M109S, and illuminated with bright light. Eyes were collected from euthanized mice and fixed in 10% formalin in PBS for 24 h at room temperature (RT) on a rocking platform, followed by paraffin sectioning. Sections (5 μm thick) were stained with hematoxylin and eosin (H&E) and imaged by a BX60 upright microscope (Olympus, Tokyo, Japan). Then, the data were processed using MetaMorph software (Molecular Devices, Sunnyvale, CA, USA). Six mice were used in each experimental group.

Detection of rod and cone photoreceptors

To detect the rod and cone photoreceptors in the retina, eyes were collected from euthanized *Abca4*$^{-/-}$*Rdh8*$^{-/-}$ mice one week after the treatment and fixed in 4% PFA for 24 h followed by their incubation in 1% PFA for 48 h at RT. The eight-μm thick cryosections prepared from fixed eyes were incubated at 37°C for 10 min, followed by hydration with PBS for 2 min. These sections were blocked with 10% normal goat serum (NGS) and 0.3% Triton X-100 in PBS for 1 h at room temperature. Then sections were stained with a mouse 1D4 anti-rhodopsin primary antibody to visualize rods and biotinylated peanut agglutinin (PNA) (1:500 dilution) to visualize cones overnight at 4°C. The next day, sections were washed with PBS, followed by the incubation with Alexa Fluor 555-conjugated goat anti-mouse secondary antibody (1:400 dilution) to detect rods and Fluor 488-conjugated streptavidin (1:500 dilution) to detect cones for 2.5 h at room temperature. Cell nuclei were stained with DAPI. Slides were coverslipped with Fluoromount-G (SouthernBiotech). The retina was imaged with the Olympus FV1200 Laser Scanning Microscope (Olympus America, Waltham, MA) and 40x/1.4 objective.

6A7 Ab bax immunoprecipitation

Immunoprecipitation of activated Bax (The N-terminus exposed Bax) was performed as previously reported.[59] Cell lysates were prepared with 1% CHAPS buffer. The cell lysates of 150 μl (5 mg/mL protein concentration) were incubated with 10 μl of 6A7 antibody-conjugated agarose

beads (sc-23959AC, Santa Cruze) at 4C for 2 h. Then, the beads were washed with the CHAPS buffer 3 times, and the immunoprecipitated Bax was eluted by incubating the beads with 50 μl of Lamili buffer at 95C for 10 min. Fifteen (15) ul of the eluted samples was subjected to Western blot. For the detection of the total Bax expression in the cell lysate, 20 μg of total protein was subjected for each lane of the gel. To detect Bax in Western blot, an anti-Bax polyclonal antibody (50599-2-IG, Protein Tech) was used.

Bax immunocytochemistry

On Day 0, iBax cells (15,000 cells/100 μL/well) were seeded in 96 well plates, On Day 1, Dox (100 ng/mL) was added together with CSMs. After 36 h of Dox addition, cells were fixed by 2% PFA and subjected to immunocytochemistry. Anti-Bax polyclonal antibody (50599-2-IG, Protein Tech) was used to detect Bax in the cells. The pictures of Bax staining (green fluorescence), mCherry expression (red fluorescence), and normal light image were taken and used to determine the percentages of cells showing punctuated Bax staining among Bax expressing cells. At least 200 cells were counted from each image. At least 3 wells were used for each condition.

Microscale thermophoresis (MST)

His-Tag labeling Kit RED-tris-NTA 2nd generation (MO-L018, Nanotemper) was used to label His-tagged Bax purchased from Creative BioMart (Catalog No. BAX-6976H, Seattle, WA). His-Bax (210 μL/mL in Phosphate Buffer Saline (PBS) (pH7.4)) was aliquoted (10 μL/tube) and kept at −80C. For RED labeling, 0.05% CHAPS PBS was used to dissolve the RED dye. The final concentration of the labeled Bax protein was 50 nM for the binding assay and was mixed with a serial dilution of CSMs. The first concentration of CSMs (20 μM) was prepared in PBS with 1% BSA and 2% NP40. The final condition of the buffer for binding was PBS with 0.5% BSA and 1% NP40 in all 16 reaction tubes. When 1% NP40 was replaced with 1% CHAPS, the dose-dependent binding signal was not detected as explained in discussion. The labeled His-Bax was kept on ice and used within 3 h after the labeling. The measurement of dissociation constant K_d was performed by the NanoTemper's software installed in the Monolith system.

Seahorse experiment

XF Cell Mito Stress test kit (103015-100) was used to measure OCR and ECAR with the XFe96 Seahorse instrument. On Day 0, the cell culture of MEFs was started (1.6×10^4 cells/200 micro-l/well (Agilent, XF96 microplate V3-PS)) using a MEF medium. On Day 1, CSMs were added to the culture medium (10 nM, 100nM, or 1 μM) and incubated for 4 h in a CO_2 incubator. After the incubation, the medium was changed with XF DMEM medium (Agilent, 103575-100), and cells were incubated in a 37°C chamber (100% air) for 1 h before the mitochondria stress test. For the test, rotenone (0.5 μM), antimycin A (0.5 μM), oligomycin (1.5 μM), and FCCP (2.0 μM) were used according to the manufacturer's protocol. OCR and ECAR were recorded and the effects of CSMs on OXPHOS and glycolysis were analyzed.

ROS measurement

ROS-Glo-H_2O_2 Assay kit (Promega G8820) was used to measure ROS in MEFs culture (medium and cells) according to the manufacturer's protocol. On day 0, cells were seeded at the concentration of 16,000 cells/100 μL/well in 96-well plate. On day 1 (24 h after the start of cell culture), cells were pre-incubated with 0.001% DMSO only (M109S 0 nM) or M109S (100 nM, 200 nM, 1 μM (the final DMSO was adjusted to 0.001% in all the conditions) for 4 h. Then, the medium was changed to a new medium containing 25 μM H2O2 substrate with DMSO or M109S (medium in each well was 100 μL). Cells were cultured in a CO_2 incubator for additional 4 h. Then, 100 μL of ROS-glo Detection solution was added to each well and incubated for 20 min at room temperature. Luminescence intensity from each well was recorded by MG3500 (Promega) plate reader.

Cell number measurement

On Day 0, the cell culture of MEFs was seeded (4×10^5 cells/mL/well (12 well plate)). On day 1, 24 h after the starting of the cell culture, the various concentration of CSMs were added to the culture medium. On Day 2, 48 h after the start, cells were collected, and cell number was counted by an automated cell counter (Countess II, Invitrogen). Four wells were used for one condition.

QUANTIFICATION AND STATISTICAL ANALYSIS

Statistical

For Figures 1, 2, 3, 4, 5, and 6, Statistical analyses and calculations of EC_{50} were performed using Prism (version 9.4.1). For all the dose-dependent effects analysis, one-way ANOVA analysis with Turkey's post hoc tests were used (Prism software was used). Student's *t* test was used to determine the statistical significance between two groups. Values of $p < 0.05$ were considered statistically significant. Data collection and statistical analysis were performed by different personnel. Data are presented as mean ± SD.